24. JOINT NASA-BRITISH MINISTRY OF TECHNOLOGY SKID CORRELATION STUDY

RESULTS FROM BRITISH VEHICLES

By R. W. Sugg

Ministry of Technology

SUMMARY

Speed friction results are given from the three British friction vehicles which were engaged in the Joint NASA-Ministry Skid Correlation Trials at NASA Wallops Station. The degree of correlation between the vehicles and aircraft is demonstrated and the ability of the equipment to place the test surfaces in the same friction order as the aircraft is discussed. An investigation is made into the ability of two of the equipments to predict aircraft stopping distances. Braking-force coefficients in the anti-skid, locked-wheel and impending-skid friction conditions are compared, also the effect of changes in tyre pressure. A comparison is made with a standard aircraft tyre prior and subsequent to the introduction of blind pin holes in the tread which were intended to provide an additional way of escape for water in the tyre-ground contact area.

INTRODUCTION

It was approximately six years ago that the Ministry of Technology first investigated the possibility of correlation between the wet friction of runways as measured by vehicles and aircraft by conducting trials with a fighter aircraft and the Road Research Laboratory Trailer. The trials report indicated that correlation was not close; but since some of the data could have been suspect because of different wetting methods, the Joint Correlation Trials at Wallops Island were most appropriate to our own friction programme and we hoped they would settle this problem.

In addition to our Runway Water Depth Monitor and Slush Drag Meter which were not engaged in the friction trial, we provided two Tapley meters and an Inertia Switch Decelerometer which were used in NASA vehicles. We also brought over the Miles Engineering Company, Ltd., version of the Road Research Laboratory Trailer; another trailer, recently developed for us by the M. L. Aviation Company, Ltd., called the Mu-Meter; and our Heavy Load Friction Vehicle, operated for us by the College of Aeronautics. This paper contains the results of the last three equipments.

The Miles Trailer (fig. 1) was designed with the primary object of producing a small, light test apparatus which could be fitted to most cars with the minimum of modification and the smallest possible effect to their stability, even when testing on extremely slippery runway surfaces. The tyre is 16 inches in diameter and 4 inches wide, and in order to provide good suspension characteristics, a wheel load of 317 lb was chosen to give a high ratio of sprung to unsprung weight. This, with the use of rubber cord springs and a hydraulic shock damper, gives excellent stability in operation throughout the speed range of over 100 mph. The trailer measures the locked-wheel braking-force coefficient and the brake is brought into action by a vacuum servo system controlled by the operator in the towing vehicle. There is no trouble from overheating or brake fade even on high-speed runs. Braking forces are measured by means of a torque arm attached to the brake, operating a strain gauge link which actuates an electronic pen recorder with a moving chart. The calibration of the apparatus is checked at frequent intervals by applying known braking forces to the trailer wheel. In addition to applying the brake the servo system also operates a clamp to prevent the trailer from swinging about the towing point while the wheel is locked because it then has little directional stability, particularly on the more slippery surfaces. To ensure consistency and reproducibility of results, particular attention has been paid to the standardisation of the physical properties of the test tyres such as hardness, resilience, area and perimeter of contact patch, and so forth.

The Mu-Meter (fig. 2) is a trailer comprising three wheels, two of which are mounted at the ends of independently movable arms pivoted to the towing eye and adjusted to a tow out angle of $7\frac{1}{2}^{o}$. When towed, the resulting side load imposed on the arms is measured by a pressure capsule mounted between them, the pressure variations being transmitted to a pen recorder which uses pressure-sensitive paper. The third wheel drives the paper chart so that a continuous record of the side load is available, this load being a measure of the surface friction. The equipment incorporates an event marker and a method of averaging friction values over any distance. It is wholly mechanical in its operation requiring no power supply. The total weight is 542 lb of which about 250 lb is removable ballast. It is 4 feet 7 inches long, 2 feet 6 inches wide, and 2 feet 10 inches high; has been towed to a speed of 115 mph; and was designed specifically to meet an ICAO requirement for a machine, which was simple to operate, to provide a continuous measurement of runway friction in a graphic form. The tyre size is 16 inches in diameter and 4 inches wide. A pressure of 10 psi is used with the intention that it should be capable of indicating when aquaplaning conditions exist at its normal towing speed of 40 mph. The tyres have no tread pattern and are rigidly controlled in their manufacture to ensure consistency of results.

The Heavy Load Friction Vehicle (fig. 3), commonly called the "Juggernaut," weighs 11 tons, is powered by a 240 bhp engine, and requires a distance of 4000 feet to reach 60 mph. The test wheel fitted with a 35 × 10-17 aircraft tyre having five circumferential ribs is located by a parallel suspension system and is mounted within the wheel base on the centre line of the vehicle just behind the front axle. This wheel is loaded through a specially developed hydraulic system by adjusting nitrogen pressure in a loading accumulator and the test load can be set to any desired value up to a maximum of 5 tons. With this ability to vary the load, tyre inflation pressures from 24 to 280 psi can be used. Drag and vertical loads are measured by strain gauges and recorded as a continuous trace. The brake is a normal aircraft plate type and can generate sufficient torque to lock on any surface encountered so far. The brake can be operated from an aircraft anti-skid system; alternatively, it can be made to lock the wheel and therefore measure the impending- and locked-wheel skid friction values. During the NASA Wallops Station study, tyre pressures of 24, 100, 160, and 280 psi were used with a normal load of 7840 lb, except that the tyre was at 24 psi when the load was 1750 lb.

RESULTS AND DISCUSSION

The trials results have been analysed to try and answer three questions:

1. Did the Convair 990, McDonnell Douglas F-4D, Miles Trailer, Mu-Meter, and Heavy Load Friction Vehicle all place the surfaces in approximately the same friction order?

2. How closely did the friction values of the ground vehicles correlate with the aircraft throughout their speed ranges?

3. How closely could a friction value at a single speed from the Miles Trailer and Mu-Meter predict aircraft stopping distance?

The answer to the first question is important as we have used the Miles type of trailer for some years to compare our military and some civil runways. This system has worked well. For example, runways complained of as being slippery by pilots were shown to be so by the trailer. There has, however, been some doubt that the aircraft and trailer corresponded except in a general way. The Mu-Meter speed-friction curves for the surfaces on Site 1 are shown in figure 4 and a few others have been added such as those for the dry surface and the Plastolene sheet we put down to simulate an icy surface. (For a description of these surfaces, see ref. 1.) The curves for all the grooved surfaces are close together at the top; there is then a gap and the curves for the low friction surfaces are together at the bottom. The aircraft indicated approximately the same trend but showed the friction of surfaces E and F to be relatively higher. An

inspection of the Mu-Meter traces for these two surfaces showed large fluctuations in friction due to ponds forming on an otherwise flat runway.

The results for the Miles Trailer on the same surfaces are in figure 5 where you will notice the upward trend in some of the curves after about 60 mph is reached. The manufacturer has explained this as being a characteristic of the type of tyre used and that it is due to its greater energy absorption on the higher textured surfaces. The phenomenon occurs to a greater or lesser extent on all types of tyre and is made use of by the designers of high-hysteresis tyres. In spite of this, the surfaces are still placed in much the same friction order as with the Mu-Meter and surface E is shown as having the lowest value, possibly for the same reason as with the Mu-Meter, that is, a variation in water depth due to ponding.

Results for the Mu-Meter and Miles Trailer on Site 1 under flooded conditions are shown in figures 6 and 7, respectively, and indicate that grooving increases the speed at which aquaplaning commences.

Curves for the Heavy Load Friction Vehicle on Site 1 using anti-skid are shown in figures 8 to 12 at tyre pressures of 100 and 160 psi and a normal load of 7800 lb. These curves demonstrate that increasing the tyre pressure reduces the friction value and that grooving not only increases the braking-force coefficient but causes it to remain level throughout the speed range. Of particular interest is surface E (Gripstop) which, although fine textured, had about the same friction characteristics as the ungrooved but more open textured asphalt (surface I).

The curves for the locked-wheel condition are in figures 13 to 21, where tyre pressures of 24, 100, 160, and 280 psi were used; the normal load was 1750 lb in the 24 psi case to keep the contact area the same as with 100 psi. The values are all lower than with anti-skid, tyre pressure having the same effect. Here again the Gripstop had similar friction characteristics to the open textured asphalt.

The curves for the impending-skid, or mu maximum, condition are in figures 22 to 30 where the friction readings are shown to be higher than in the anti-skid condition. The usual tendencies of tyre pressure and surface are apparent.

None of the three equipments placed the nine surfaces in exactly the same order as the aircraft; however, as the latter indicated a friction difference of only 0.05 between surfaces B, C, G, and H, that is all the grooved surfaces, the light trailers could not be expected to agree exactly. They did, however, place them well above the other surfaces A, D, E, F, and I. On the lower friction surfaces both trailers showed A, D, F, and E to be close together whilst the aircraft and Heavy Load Friction Vehicle showed E and F to be clearly superior to A and D; this may be due to excess water on the test

surfaces. In general, both trailers indicate the good and poor surfaces to a degree which is probably adequate for airfield classification purposes.

We now come to the second question, which is: How closely did the friction values of the ground vehicles correlate with the aircraft? There are a number of ways in which this has been determined in the past and the one chosen here is to plot speed against the ratio of vehicle to aircraft friction at the same speed. Figure 31 shows the variation in this relationship between the anti-skid values of the Heavy Load Friction Vehicle and the Convair 990, both at the same tyre pressure of 160 psi. As any lack in correlation might be thought to be due to the different anti-skid systems in use, that is, Maxaret on the Heavy Load Friction Vehicle and Hytrol on the aircraft, figure 32 uses the vehicle impending-skid values in the ratio. Correlation appears to be worse, but in general, closer agreement was achieved with the higher friction surfaces. It is of interest that the Heavy Load Friction Vehicle gave consistently higher friction values than the aircraft.

The Miles Trailer and Mu-Meter correlations were dealt with in the same way and are shown in figures 33 and 34. As with the Heavy Load Friction Vehicle it was the low friction surfaces which were inconsistent. Although it is well appreciated that the trials did not permit otherwise, it is not entirely fair to compare friction values between two systems unless they were taken under conditions of wetness which were known to be identical and within a few weeks of each other to avoid seasonal changes in friction. Our own trials in the United Kingdom have demonstrated that the amount of water on a surface is of prime importance particularly on the finer textured surfaces. Certainly some of the runs with the Mu-Meter had a trace where the friction value oscillated between 0.1 and 0.3 at 40 mph on a so-called damp runway where ponds at least 1/8 inch deep had formed; whilst during the rain which occurred early in the Wallops trial, a value of 0.8 was obtained on the same surface at the same speed. Limited trials with both trailers indicated that when patterned tyres were used, the effect of overwetting fine textured surfaces was reduced.

The third and last question – How closely could a friction value at a single speed from the Miles Trailer and Mu-Meter predict aircraft stopping distance? – is an attempt to determine if empirical relationships can be established between vehicles and aircraft. If some agreement could be demonstrated on two aircraft it would give some confidence that it was possible on others, but might introduce a system where each type of aircraft had to be tested separately on high and low friction surfaces. Bearing in mind the tyre pressures of these two trailers (Miles Trailer, 20 psi and Mu-Meter, 10 psi), speeds were chosen which were at about the "aquaplaning" velocities on the more slippery surfaces as demonstrated in the flooded trials. The speeds selected were 55 mph for the Miles Trailer and 45 mph for the Mu-Meter.

First a system was tried by making an assumption that the mean friction value for the Convair 990 was at 80 knots when stopping from 125 knots, and this value was plotted against both trailers. There was a general but not sufficiently accurate correlation – surfaces E and F were again inconsistent particularly in the flooded condition – but since the friction value for the aircraft would not necessarily be at 80 knots on all surfaces, it was discarded in favour of plotting the trailer values against aircraft stopping distances calculated from friction-speed curves. The degree of correlation by using this system is shown in figures 35 and 36 for the Mu-Meter and Miles Trailer, respectively; surfaces E and F are once again the exception to the rule and have been ignored.

In another method of predicting aircraft stopping distances by vehicles which has been suggested by NASA researchers, the ratios of wet to dry stopping distances for the aircraft and vehicle are plotted against each other for a series of surfaces. Figures 37 and 38 demonstrate the degree of correlation by calculating the stopping distances wet and dry from the speed-friction graphs for the Miles Trailer and Mu-Meter from a speed of 70 mph and comparing them with the wet-dry ratio for the 990 and F-4D from 140 knots. Surfaces E and F have been ignored for the reasons stated previously. Although some agreement has been obtained, further trials with aircraft are essential before sufficient confidence can be placed in the method.

As mentioned before, to build up sufficient data to produce these correlation curves will require trials on different friction surfaces and perhaps be too expensive. It may be thought more profitable, particularly in the civil field, merely to allocate friction numbers where the meters will denote "good," "medium," or "poor" surfaces, which is a system recommended at the ICAO conference in Montreal about a year ago. Provided different equipments were correlated to give the same word description, then it would not matter what was used and the pilot would come to understand what each description meant to his aircraft. These Wallops Station trials may be instrumental in demonstrating what correlation exists between various friction-measuring equipments.

Figures 39 to 61 show friction curves for the three vehicles on Site 2 (ref. 1); the Heavy Load Friction Vehicle only tested a percentage of these surfaces, all in the locked-wheel and impending-skid condition. The usual trends were apparent: increase in friction with a reduction in tyre pressure at the same normal load, impending values higher than locked wheel, and an increase in friction due to grooves.

At 100 psi the Heavy Load Friction Vehicle showed little difference between longitudinally and transversely grooved concrete. Transverse grooves in asphalt were, however, shown to be superior to longitudinal and an improvement in friction was achieved by reducing the groove pitch from 1 inch to 3/4 inch. The Sinopal gave results which were better than some grooved surfaces, appeared to have good speed characteristics, and was as effective as the transversely grooved and ungrooved concrete.

The Miles Trailer showed the transversely grooved concrete to be superior to longitudinal grooves and the Sinopal to be inferior to grooved concrete. The poor results on the Sinopal may have been due to the trailer measuring the friction of the black filler and not the Sinopal itself. The optimum surface was the original open textured asphalt in Area B of Site 2 although the transversely grooved concrete was marginally superior at 80 mph. The poorest results were obtained from the Eastern Shore sand mix. The curves for asphalt, epoxy, and grooved concrete all showed rising curves at speeds above approximately 40 to 60 mph. The remainder showed a decaying friction. The synthetic surface, Sinopal, gave a decreasing result but was better than epoxy, original concrete, Eastern Shore sand mix, or longitudinally grooved concrete for speeds up to 60 mph.

The Mu-Meter showed little difference between transversely and longitudinally grooved concrete and asphalt. The 1-inch pitch grooved asphalt was inferior to the 3/4-inch pitch and again the open textured asphalt in area D was among the best, being as good as the grooved surfaces at high speed. The epoxy, Carrier Deck Paint, and Sinopal surfaces gave very good values at low speed but appeared to be dropping rather sharply at 80 mph. Again the worst surface was the Eastern Shore sand mix which did not have good high- or low-speed characteristics.

As an entirely separate trial, the Heavy Load Friction Vehicle was used to compare the friction characteristics of a standard aircraft tyre with those of some tyres provided by the Dunlop Rubber Company with blind pin holes drilled in the tread.

The reasoning behind this modification is that in order to develop a retarding force on wet runways, the water film must be excluded from at least a portion of the tyre-runway contact area. The total time that any one point on the tyre takes to go through the contact area is governed by speed and deflection; this can be very short, in the order of 10 milliseconds. Within this time it is suggested that a three-stage process occurs (fig. 62):

1. In the first stage, the bulk of the water has to move sideways outside the path of the tyre or into the tread grooves.

2. The second stage is an intermediate one when the finer asperities constituting the runway microtexture start breaking through the water film.

3. The third and last stage is when the thin water film is squeezed from between the tyre tread and runway surface.

It is in the second and particularly the third stage of this cycle that the drag forces are developed. The speed with which water is removed from the contact area is therefore of prime importance and can be increased by having an open textured surface and a tread pattern with sufficient drainage channels. Unfortunately the high tangential forces with aircraft tyres at the ground-tyre interface would cause tread damage in the form of

tearing and chunking if any of the well established types of fragmentated tread patterns were used under dry braking conditions. The addition of a large number of blind pin holes in the tread to provide an additional way of escape for the water in the contact area does not incur any of these disadvantages. (See fig. 62.) Figures 63 to 69 compare the friction of modified and unmodified tyres and it appears that in general on the finer textured surfaces the modified tyre gave an increase in friction particularly at the higher speeds.

It is intended that we will conduct aircraft trials in the United Kingdom to investigate the full capabilities of this type of tyre.

CONCLUSIONS

During the tests with the trailers under so-called damp conditions there was too much water on the surface which formed puddles despite efforts at removal by sweeping. This caused them to record large fluctuations in friction particularly on the lower friction surfaces and possibly resulted in some friction coefficients being lower than under normal wet conditions. The two trailers demonstrated that they were capable of classifying the runway surfaces on Site 1 in the same general order as the Convair 990 and McDonnell Douglas F-4D. The ratio on the Miles Trailer friction readings to those of the 990 on the nine surfaces of Site 1 lay between 1.2 and 2.0 at 20 mph and 0.3 and 1.8 at 80 mph. The ratio of the friction readings of the Mu-Meter to those of the 990 under the same conditions lay between 1.2 and 2.8 at 20 mph and 0.2 and 1.8 at 100 mph. The friction ratio of the Heavy Load Friction Vehicle with impending skid to the 990 on the same surfaces lay between 1.4 and 2.1 at 20 mph and between 1.6 and 3.0 at 60 mph. In the anti-skid braking condition the ratio was between 1.1 and 1.5 at 20 mph and 1.2 and 2.1 at 60 mph.

Except for two of the surfaces, there was a fair degree of correlation between the friction values of the Miles Trailer and Mu-Meter at 55 and 40 mph, respectively, with the 990 and F-4D stopping distances. Tests on the flooded surfaces with the trailers indicate that the speed at which aquaplaning begins increases with the more open textured or grooved surfaces.

All three test vehicles demonstrated that the 1- by 1/4- by 1/4-inch grooving at least doubled the friction coefficient of the surfaces. Longitudinal grooving was less effective than lateral, and reducing the pitch of the grooves from 1 inch to 3/4 inch appeared to make little difference. The open textured asphalt on Site 2 (Section 2, Area B), which consisted of large stones set in a fine aggregate, was as effective as 1/8-inch grooved asphalt or concrete. The epoxy and Sinopal surfaces did not appear to have any friction advantages over the concrete or asphalt and were sometimes less

effective when the latter were grooved, particularly at the higher speeds. It was noted that as the trial proceeded, the black filler wore off the Sinopal so that the friction being measured may have been that of the filler and not the aggregate.

With the Heavy Load Friction Vehicle a reduction in tyre pressure with the same normal load increased the friction values. Reducing the normal load to keep the tyre footprint area the same also increased the friction value.

The concrete surfaces, grooved or ungrooved, were in general slightly lower in friction than asphalt. The Carrier Deck Paint had good friction properties at speeds up to 60 mph, but the Eastern Shore sand mix had poor characteristics and was probably the lowest in friction of all the surfaces tested.

The introduction of blind pin holes in the tyre tread appears to increase the friction on the more slippery surfaces and reduce it on grooved surfaces.

REFERENCE

1. Horne, Walter B.: Results From Studies of Highway Grooving and Texturing at NASA Wallops Station. Pavement Grooving and Traction Studies, NASA SP-5073, 1969. (Paper No. 26 herein.)

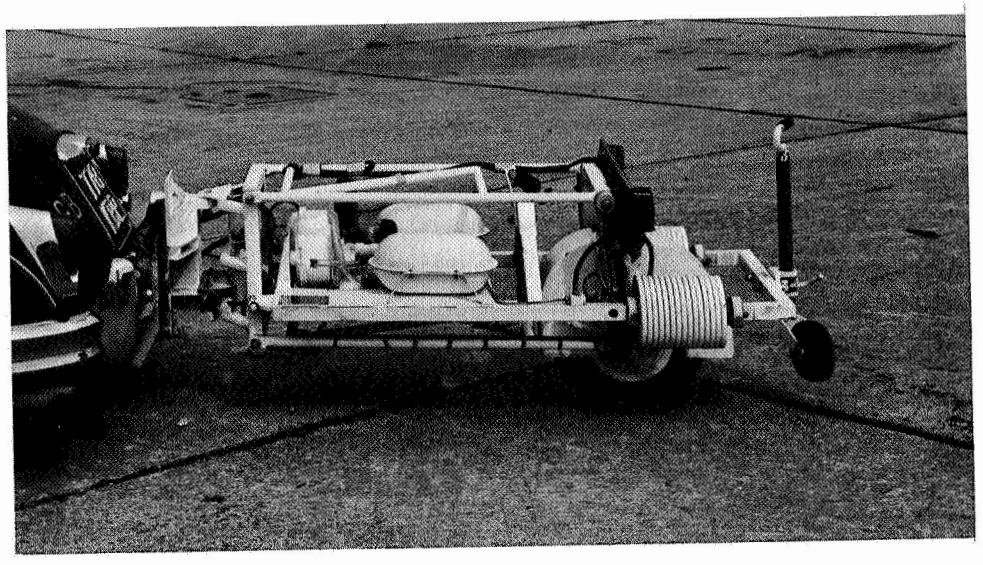

Figure 1.- Miles Trailer.

Figure 2.- Mu-Meter.

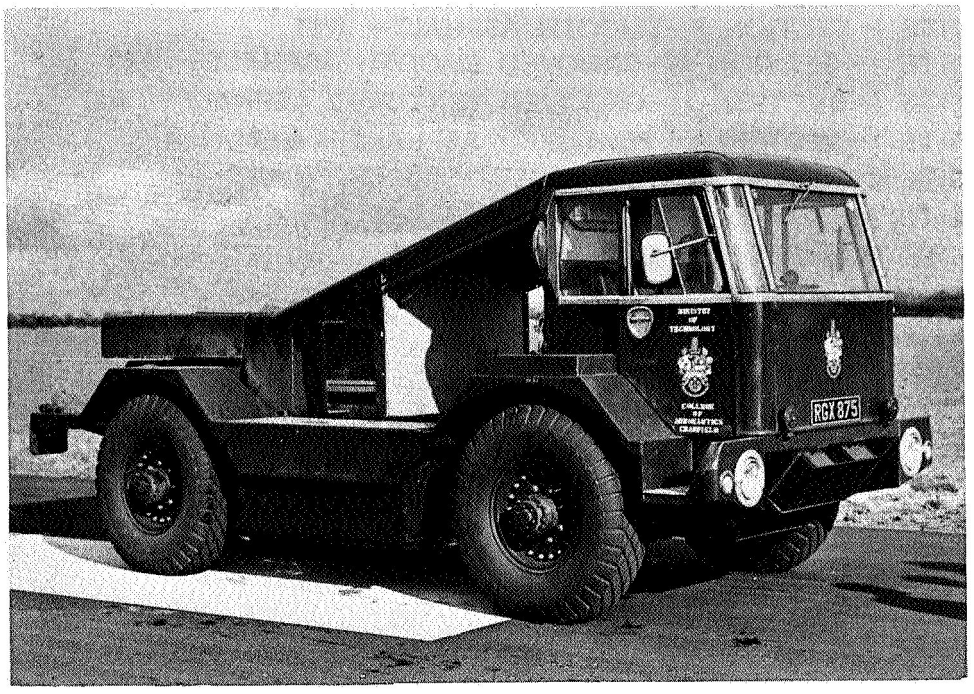

Figure 3.- Heavy Load Friction Vehicle.

1 SITE 1-SECTION A-SMOOTH CONCRETE- WET
2 SITE 1-SECTION B-GROOVED SMOOTH CONCRETE — WET
3 SITE 1-SECTION C-GROOVED TEXTURED CONCRETE- WET
4 SITE 1-SECTION D-TEXTURED CONCRETE- WET
5 SITE 1-SECTION E-GRIPSTOP- WET
6 SITE 1-SECTION F-SMOOTH ASPHALT- WET
7 SITE 1-SECTION G-GROOVED SMOOTH ASPHALT- WET
8 SITE 1-SECTION H-GROOVED TEXTURED ASPHALT- WET
9 SITE 1-SECTION I-TEXTURED ASPHALT- WET
10 SITE 2-SECTION 5-⅛" GROOVED ASPHALT- WET
11 SITE 2-SECTION -PLASTOLENE - WET
12 SITE 1-SECTION B-GROOVED SMOOTH CONCRETE-DRY

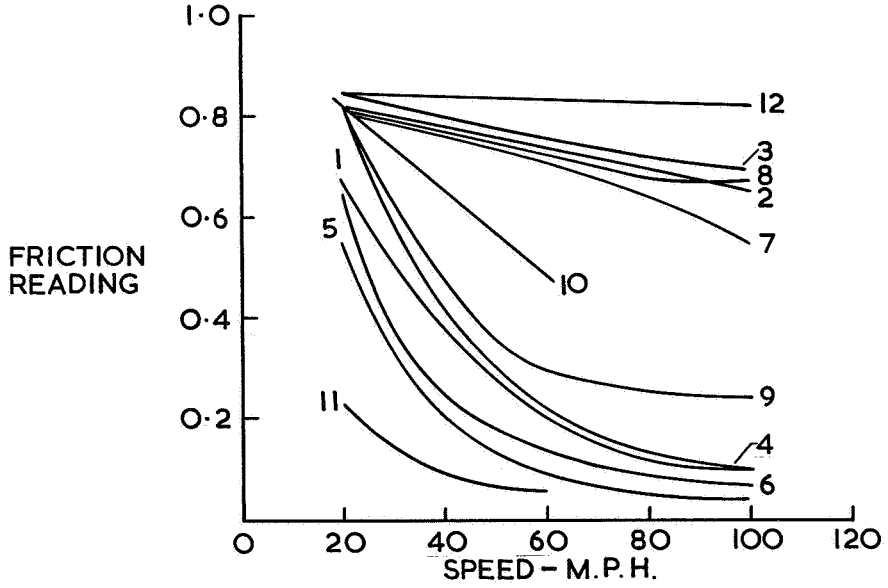

Figure 4.- Mu-Meter comparison of surfaces.

1 SITE 1-SECTION A-SMOOTH CONCRETE— WET
2 SITE 1-SECTION B-GROOVED SMOOTH CONCRETE — WET
3 SITE 1-SECTION C-GROOVED TEXTURED CONCRETE— WET
4 SITE 1-SECTION D-TEXTURED CONCRETE— WET
5 SITE 1-SECTION E-GRIPSTOP — WET
6 SITE 1-SECTION F-SMOOTH ASPHALT— WET
7 SITE 1-SECTION G-GROOVED SMOOTH ASPHALT — WET
8 SITE 1-SECTION H-GROOVED TEXTURED ASPHALT — WET
9 SITE 1-SECTION I-TEXTURED ASPHALT — WET
10 SITE 2-SECTION 5-⅛" GROOVED ASPHALT - WET
11 SITE 2-SECTION -PLASTOLENE - WET
12 SITE 1-SECTION B-GROOVED SMOOTH CONCRETE-DRY

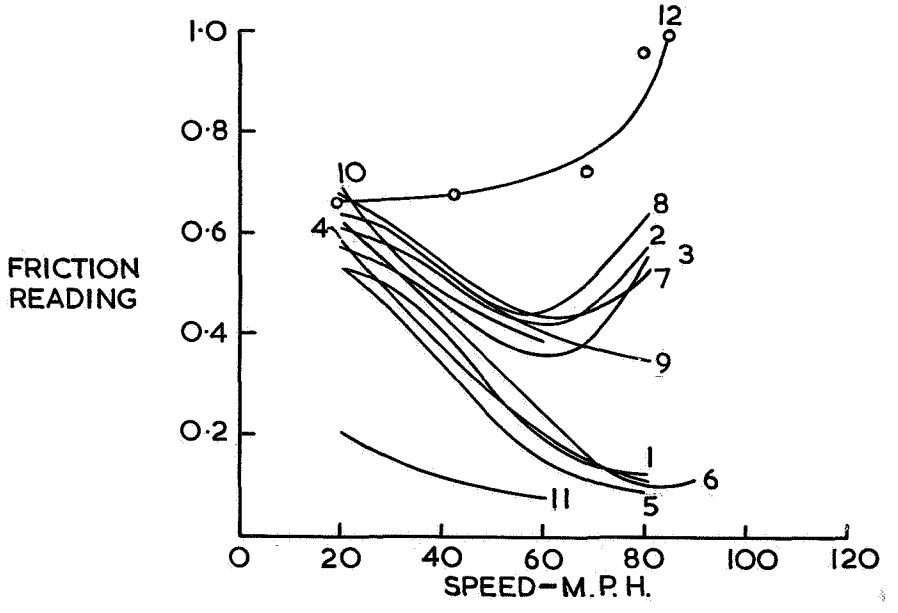

Figure 5.- Miles Trailer comparison of surfaces.

1 SITE 1 - SECTION A - FINE TEXTURED CONCRETE - FLOODED
2 SITE 1 - SECTION B - GROOVED SMOOTH CONCRETE - FLOODED
3 SITE 1 - SECTION C - GROOVED TEXTURED CONCRETE - FLOODED
4 SITE 1 - SECTION D - TEXTURED CONCRETE - FLOODED
5 SITE 1 - SECTION E - GRIPSTOP - FLOODED
6 SITE 1 - SECTION F - SMOOTH TEXTURED ASPHALT - FLOODED
7 SITE 1 - SECTION G - GROOVED SMOOTH ASPHALT - FLOODED
8 SITE 1 - SECTION H - GROOVED TEXTURED ASPHALT - FLOODED
9 SITE 1 - SECTION I - TEXTURED ASPHALT - FLOODED

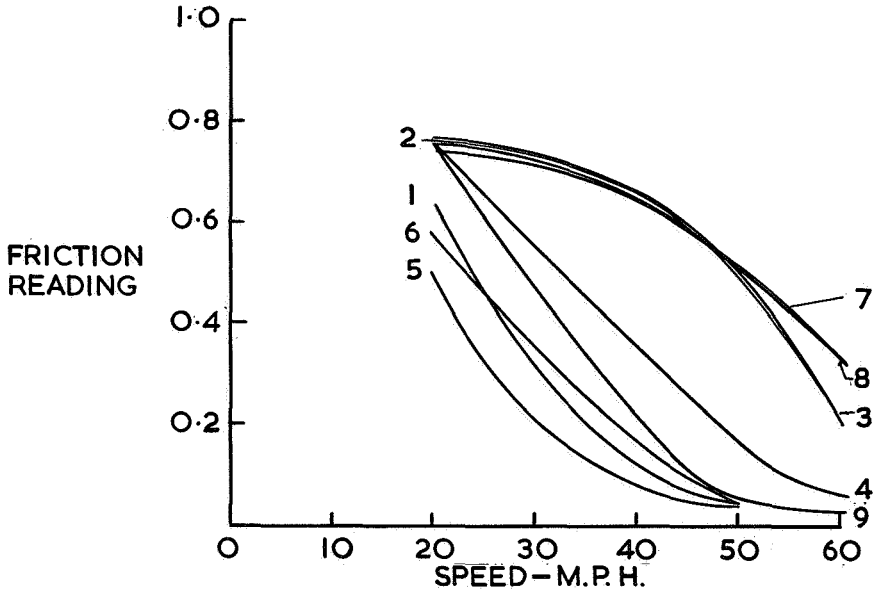

Figure 6.- Comparison of surfaces. Site 1; flooded; Mu-Meter.

1 SITE 1 - SECTION A - FINE TEXTURED CONCRETE - FLOODED
2 SITE 1 - SECTION B - GROOVED SMOOTH CONCRETE - FLOODED
3 SITE 1 - SECTION C - GROOVED TEXTURED CONCRETE - FLOODED
4 SITE 1 - SECTION D - TEXTURED CONCRETE - FLOODED
5 SITE 1 - SECTION E - GRIPSTOP - FLOODED
6 SITE 1 - SECTION F - SMOOTH TEXTURED ASPHALT - FLOODED
7 SITE 1 - SECTION G - GROOVED SMOOTH ASPHALT - FLOODED
8 SITE 1 - SECTION H - GROOVED TEXTURED ASPHALT - FLOODED
9 SITE 1 - SECTION I - TEXTURED ASPHALT - FLOODED

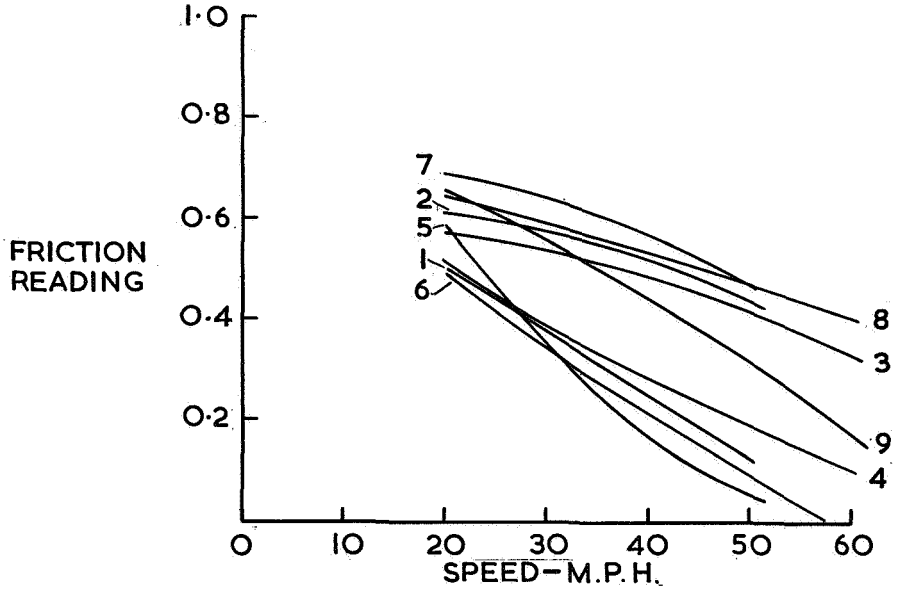

Figure 7.- Comparison of surfaces. Site 1; flooded; Miles Trailer.

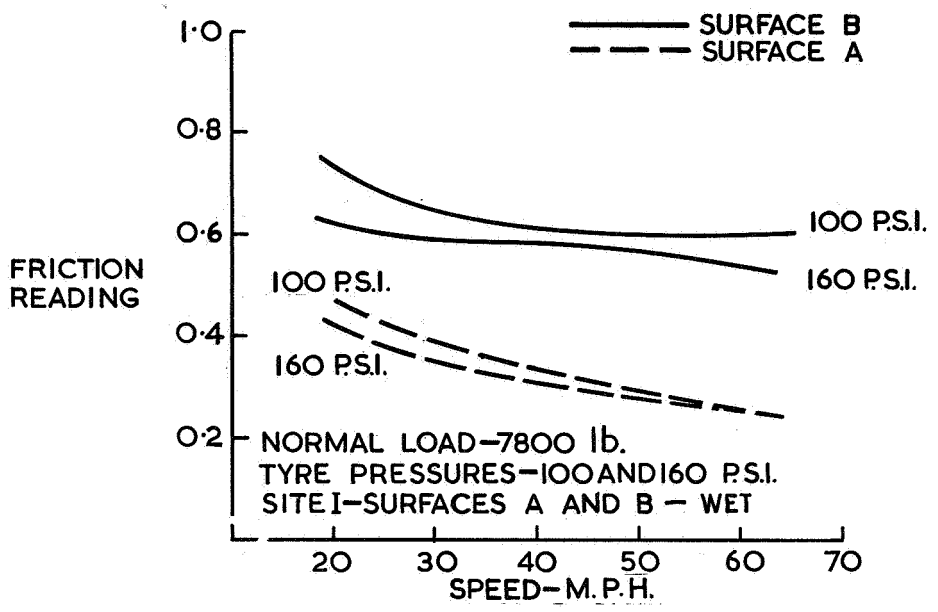

Figure 8.- Relationship between anti-skid braking-force coefficient and speed with Heavy Load Friction Vehicle. Surfaces A and B.

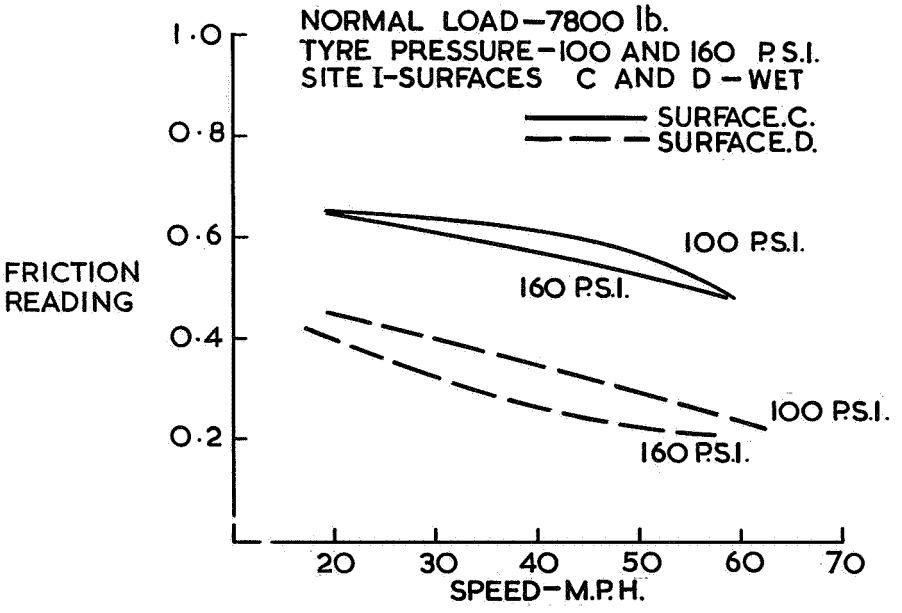

Figure 9.- Relationship between anti-skid braking-force coefficient and speed with Heavy Load Friction Vehicle. Surfaces C and D.

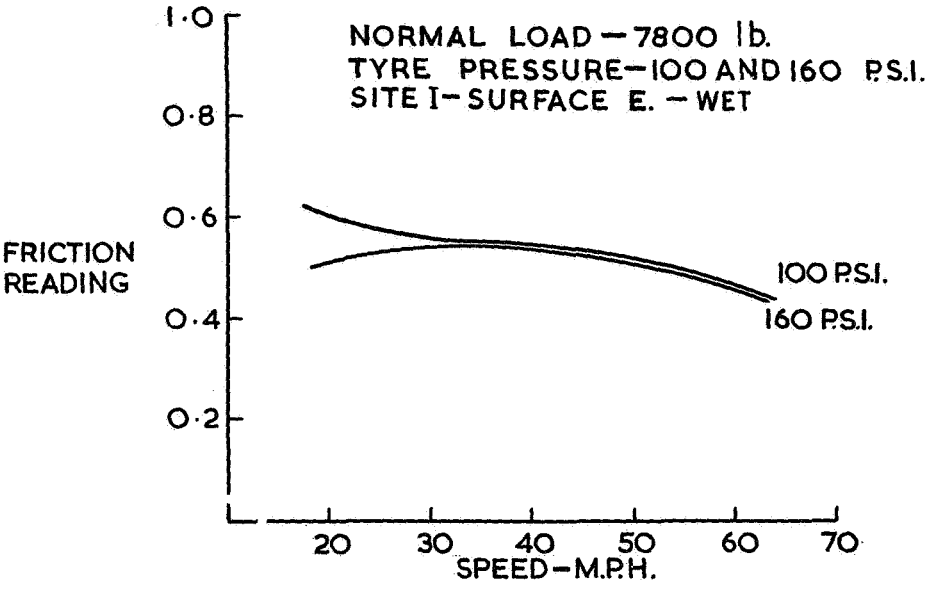

Figure 10.- Relationship between anti-skid braking-force coefficient and speed with Heavy Load Friction Vehicle. Surface E.

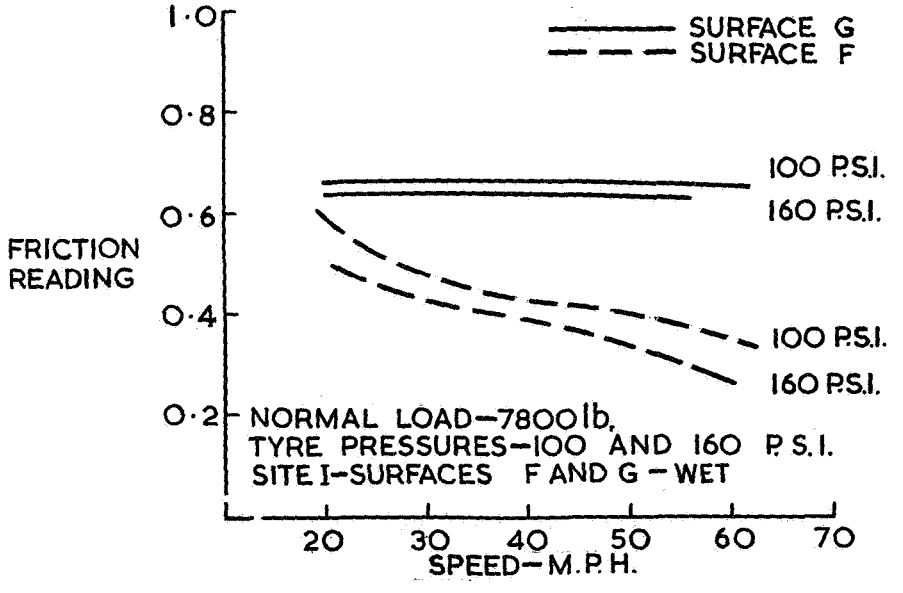

Figure 11.- Relationship between anti-skid braking-force coefficient and speed with Heavy Load Friction Vehicle. Surfaces F and G.

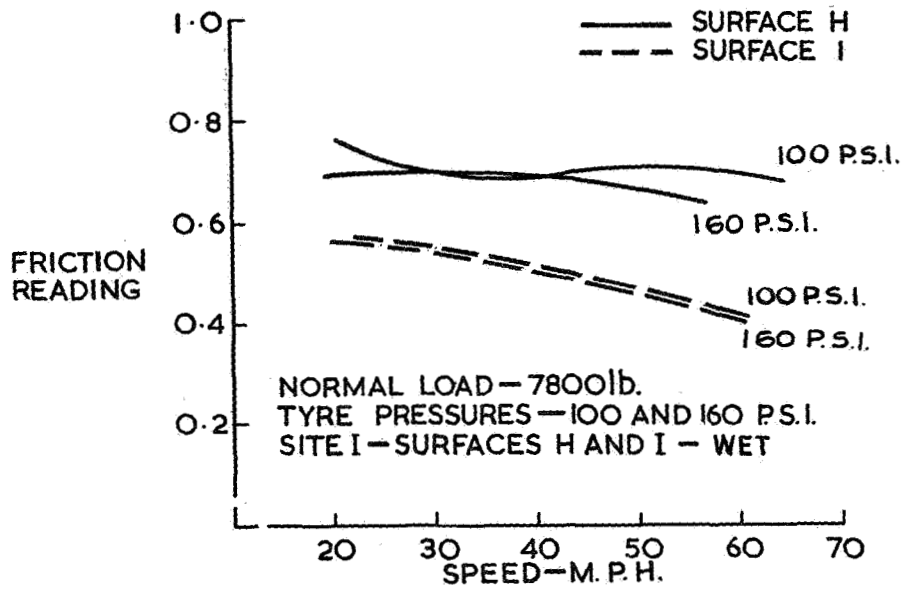

Figure 12.- Relationship between anti-skid braking-force coefficient and speed with Heavy Load Friction Vehicle. Surfaces H and I.

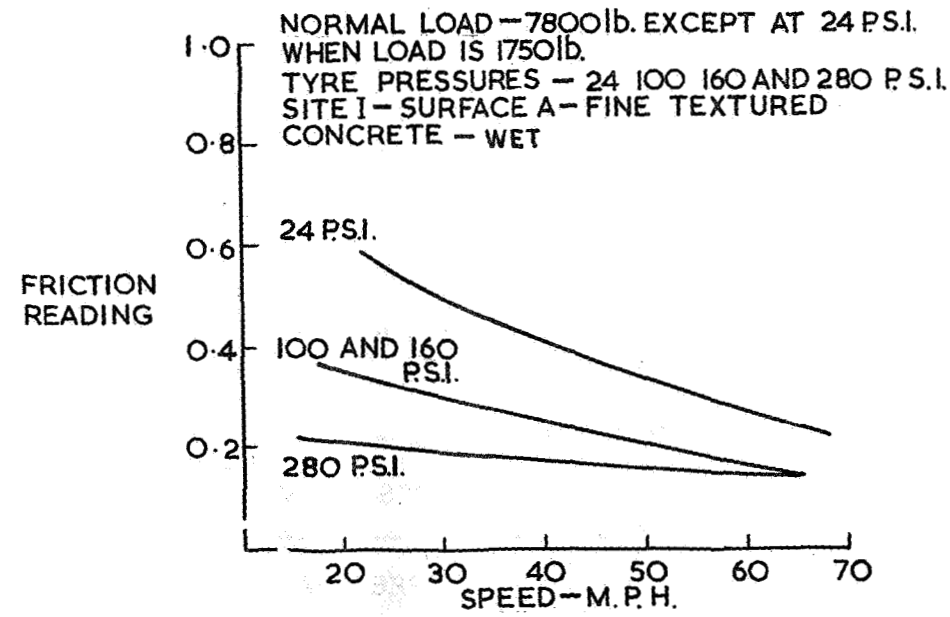

Figure 13.- Relationship between locked-wheel braking-force coefficient and speed with Heavy Load Friction Vehicle. Surface A.

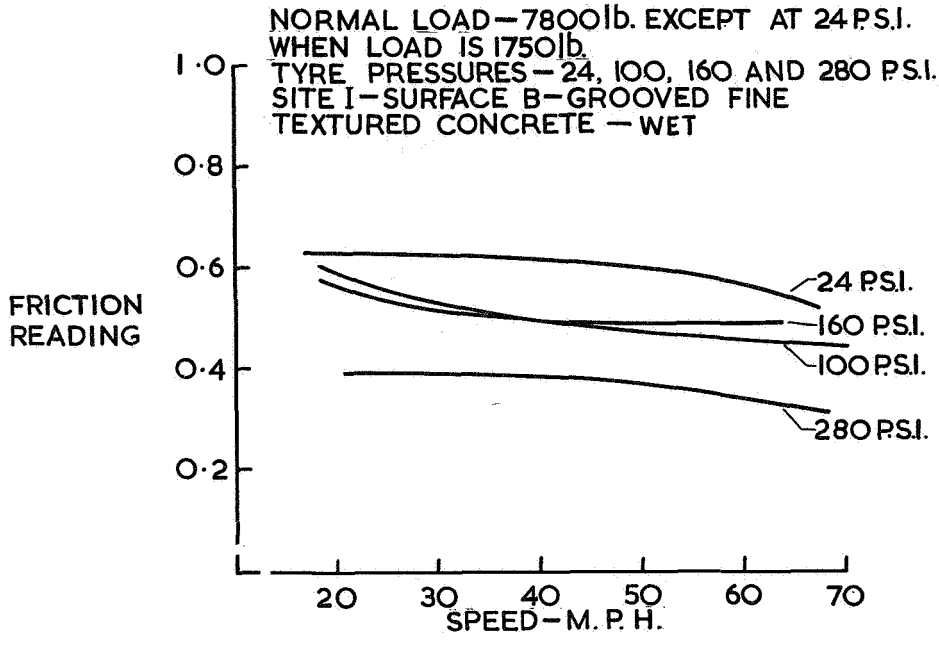

Figure 14.- Relationship between locked-wheel braking-force coefficient and speed with Heavy Load Friction Vehicle. Surface B.

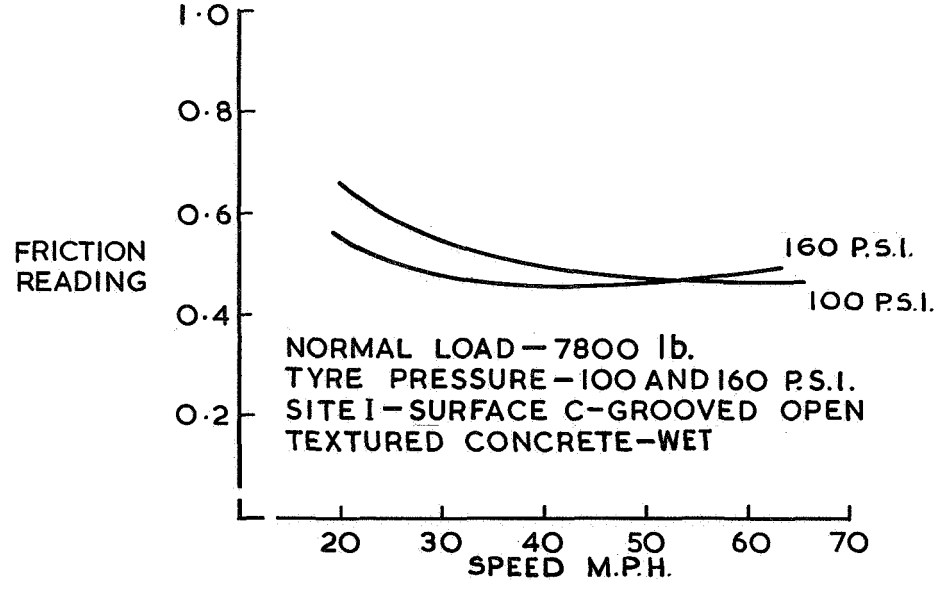

Figure 15.- Relationship between locked-wheel braking-force coefficient and speed with Heavy Load Friction Vehicle. Surface C.

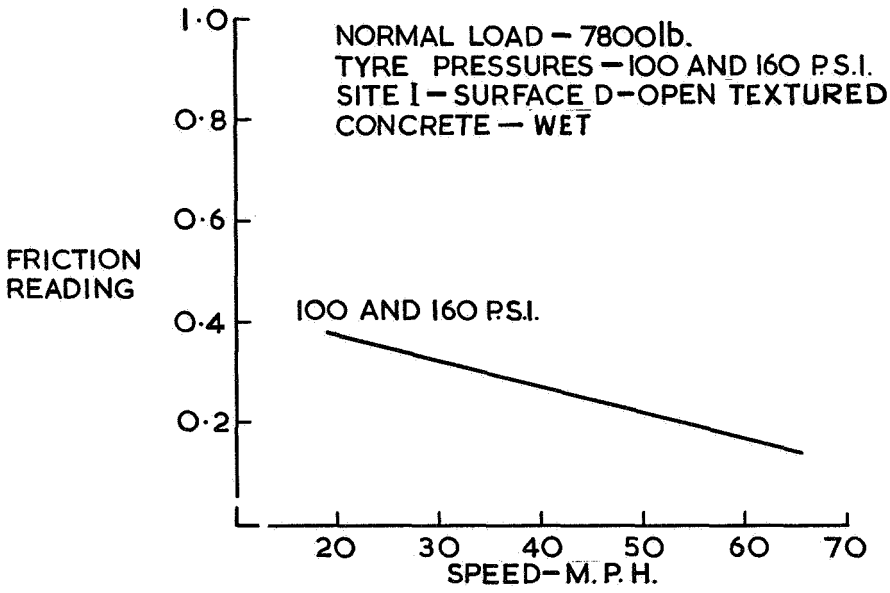

Figure 16.- Relationship between locked-wheel braking-force coefficient and speed with Heavy Load Friction Vehicle. Surface D.

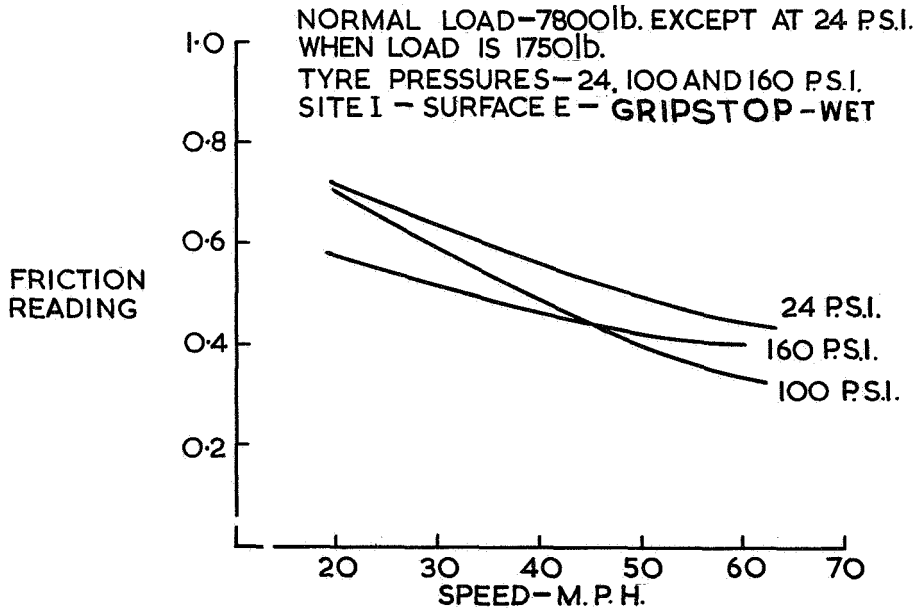

Figure 17.- Relationship between locked-wheel braking-force coefficient and speed with Heavy Load Friction Vehicle. Surface E.

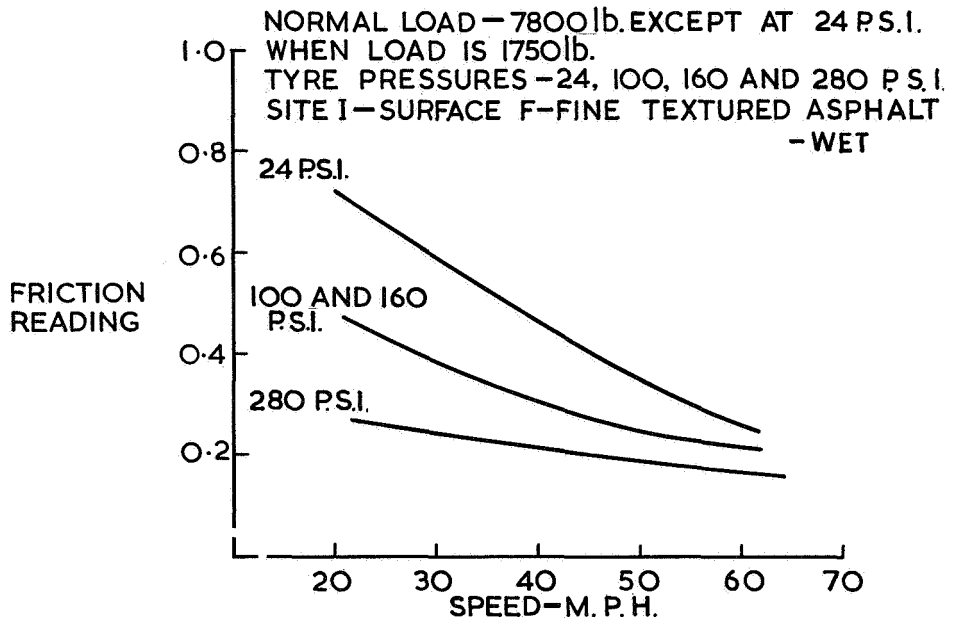

Figure 18.- Relationship between locked-wheel braking-force coefficient and speed with Heavy Load Friction Vehicle. Surface F.

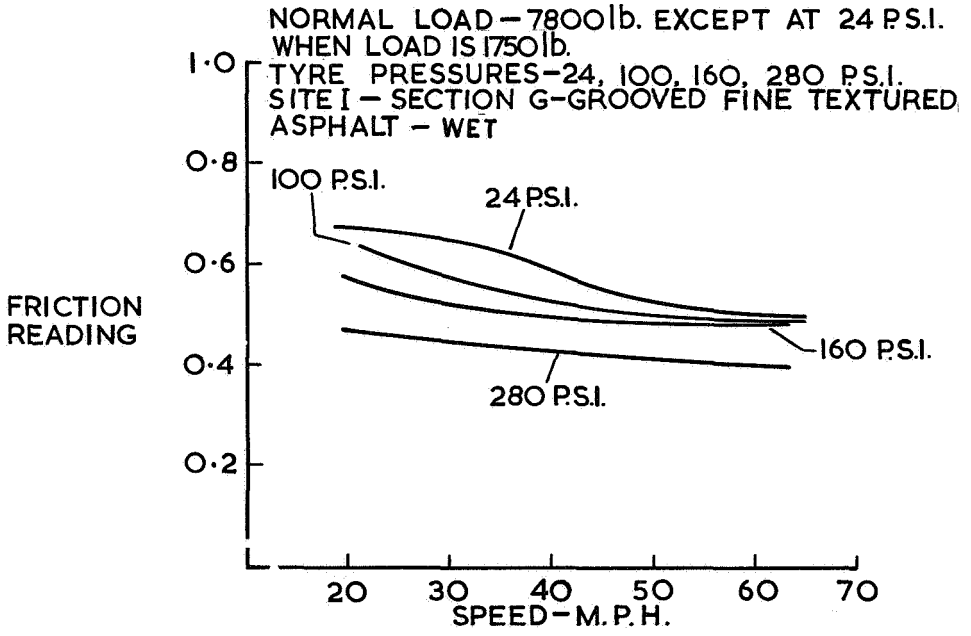

Figure 19.- Relationship between locked-wheel braking-force coefficient and speed with Heavy Load Friction Vehicle. Surface G.

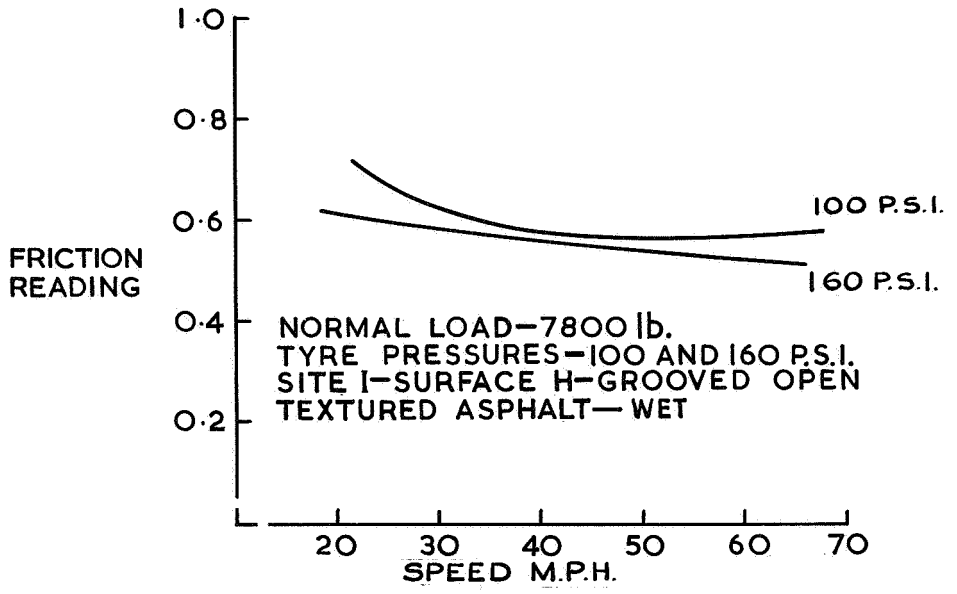

Figure 20.- Relationship between locked-wheel braking-force coefficient and speed with Heavy Load Friction Vehicle. Surface H.

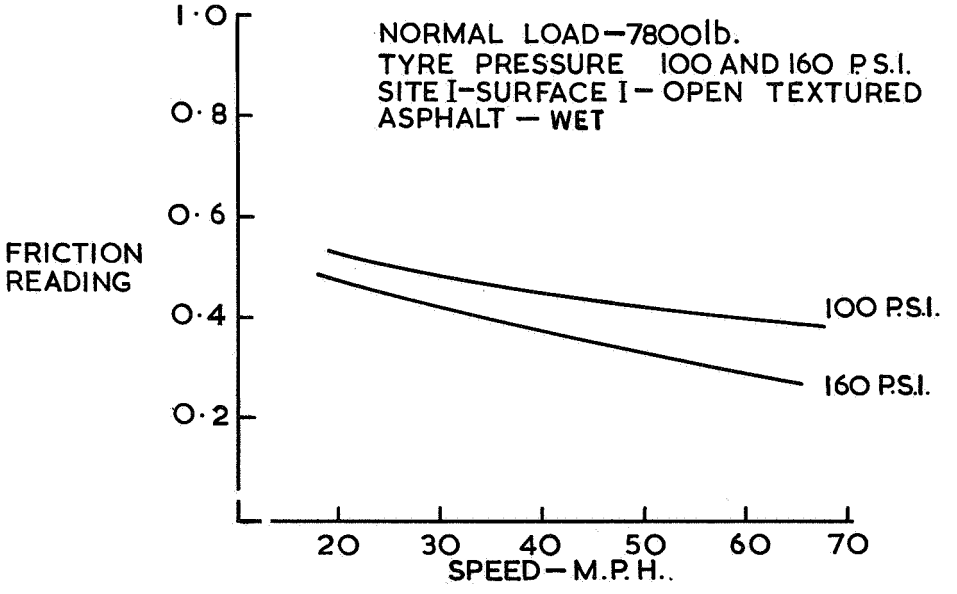

Figure 21.- Relationship between locked-wheel braking-force coefficient and speed with Heavy Load Friction Vehicle. Surface I.

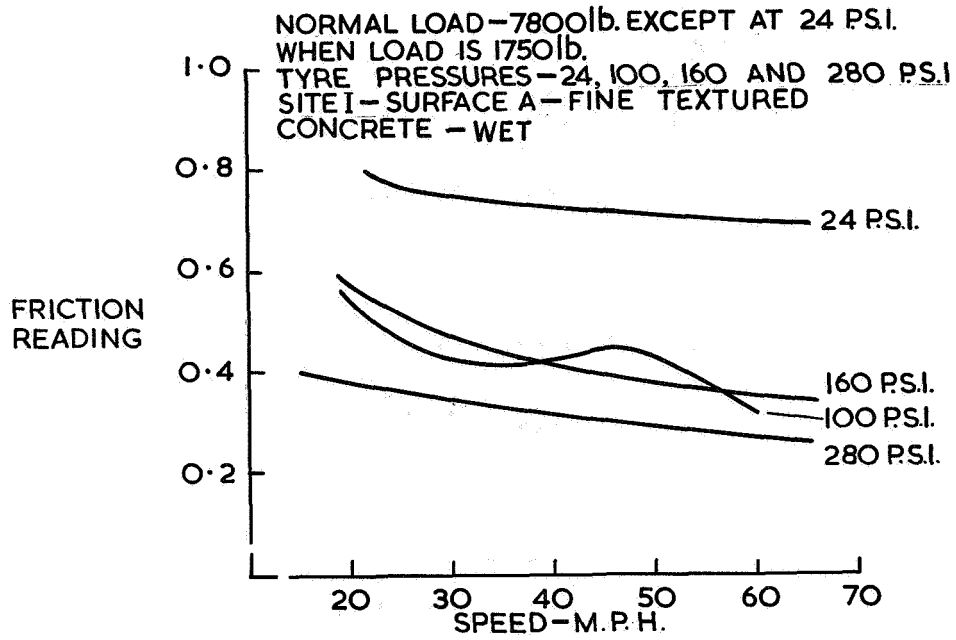

Figure 22.- Relationship between impending-skid braking-force coefficient and speed with Heavy Load Friction Vehicle. Surface A.

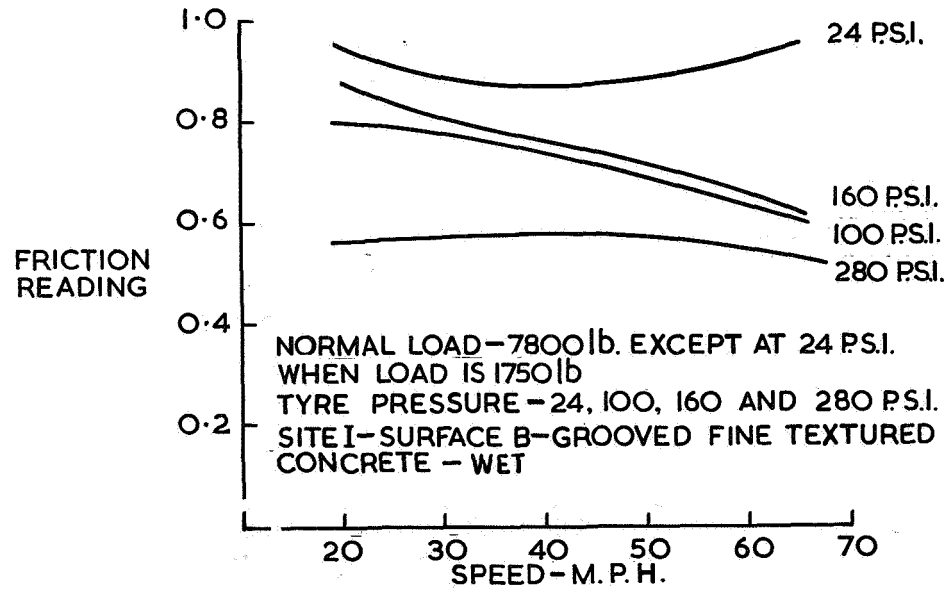

Figure 23.- Relationship between impending-skid braking-force coefficient and speed with Heavy Load Friction Vehicle. Surface B.

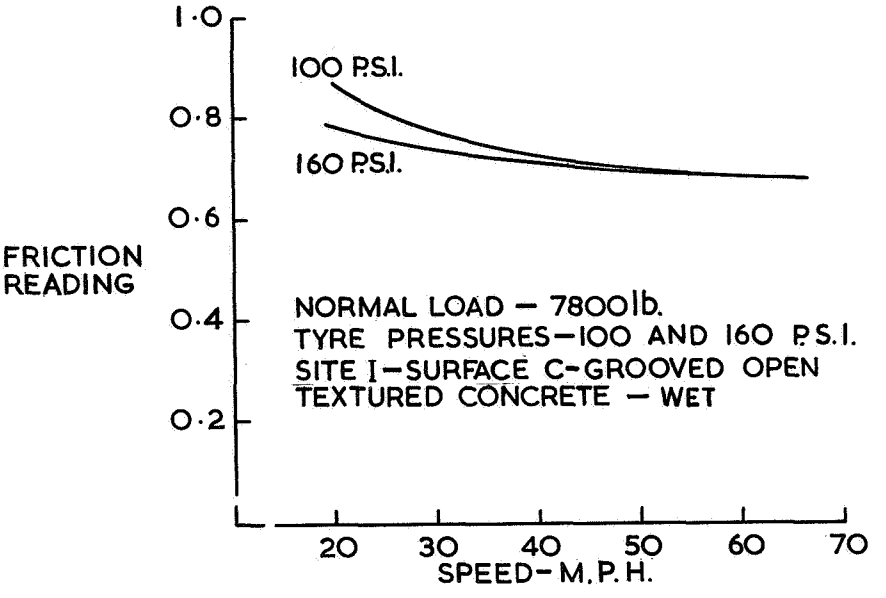

Figure 24.- Relationship between impending-skid braking-force coefficient and speed with Heavy Load Friction Vehicle. Surface C.

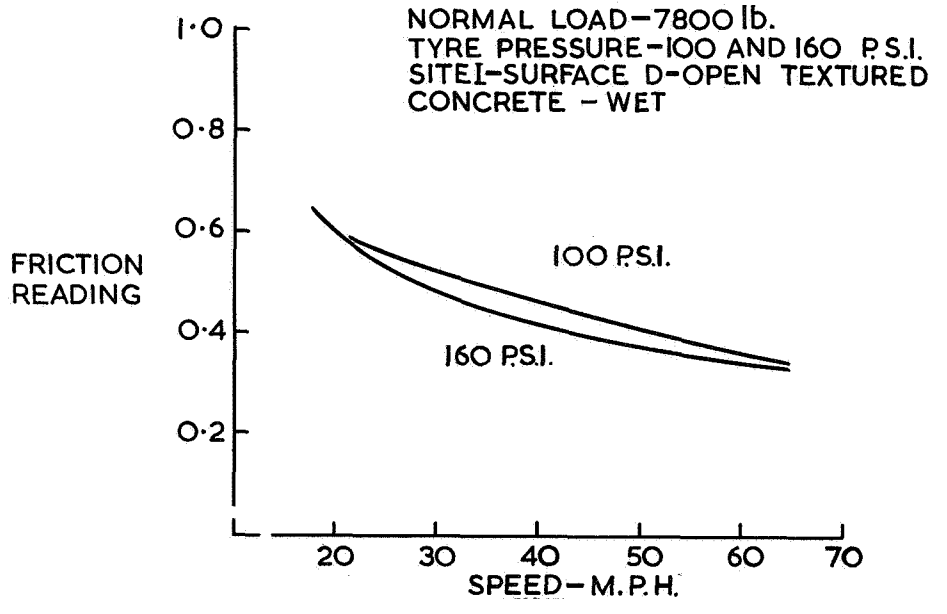

Figure 25.- Relationship between impending-skid braking-force coefficient and speed with Heavy Load Friction Vehicle. Surface D.

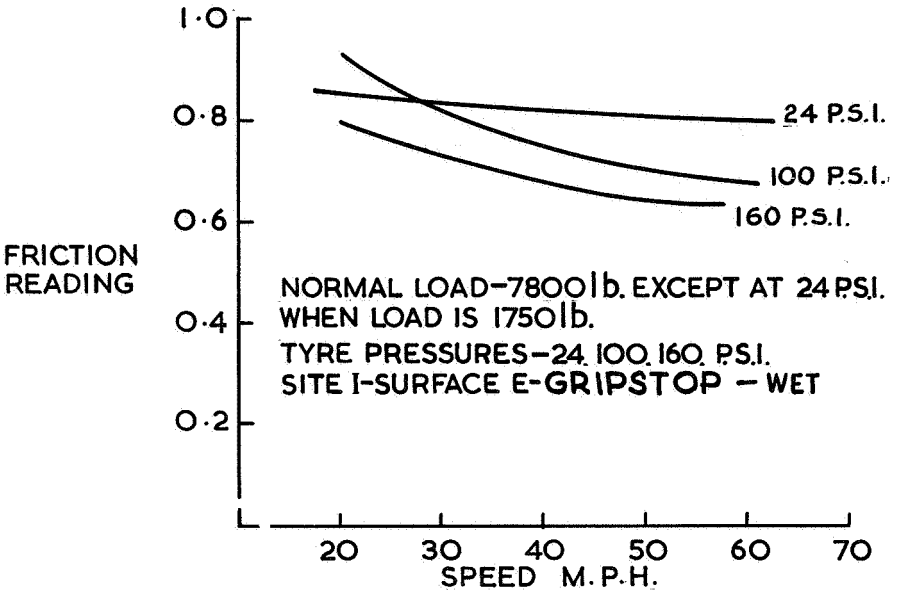

Figure 26.- Relationship between impending-skid braking-force coefficient and speed with Heavy Load Friction Vehicle. Surface E.

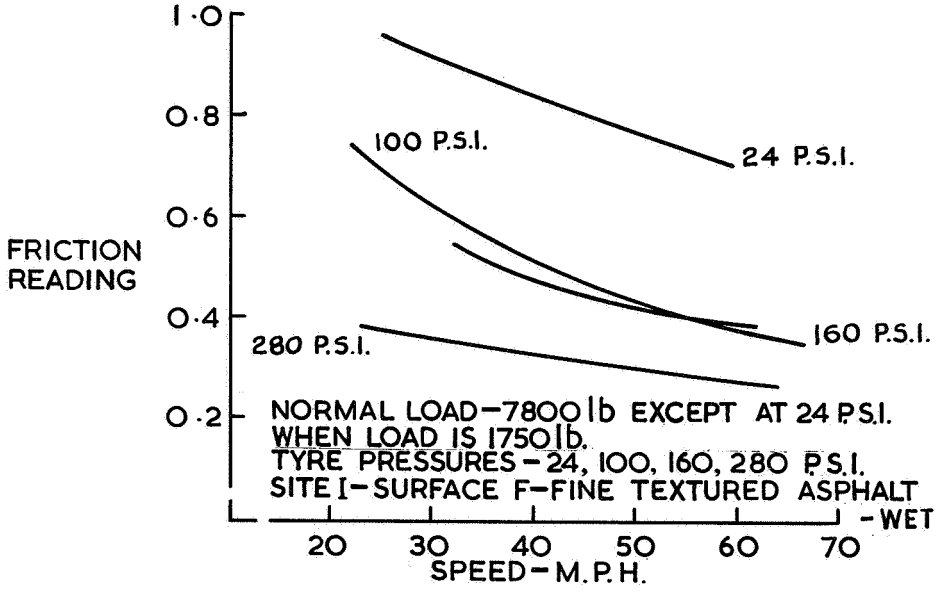

Figure 27.- Relationship between impending-skid braking-force coefficient and speed with Heavy Load Friction Vehicle. Surface F.

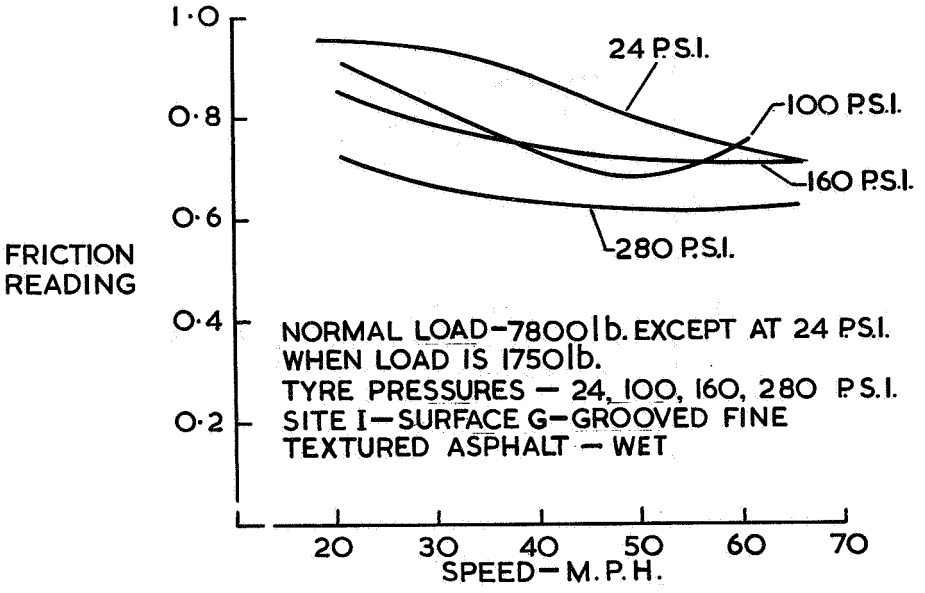

Figure 28.- Relationship between impending-skid braking-force coefficient and speed with Heavy Load Friction Vehicle. Surface G.

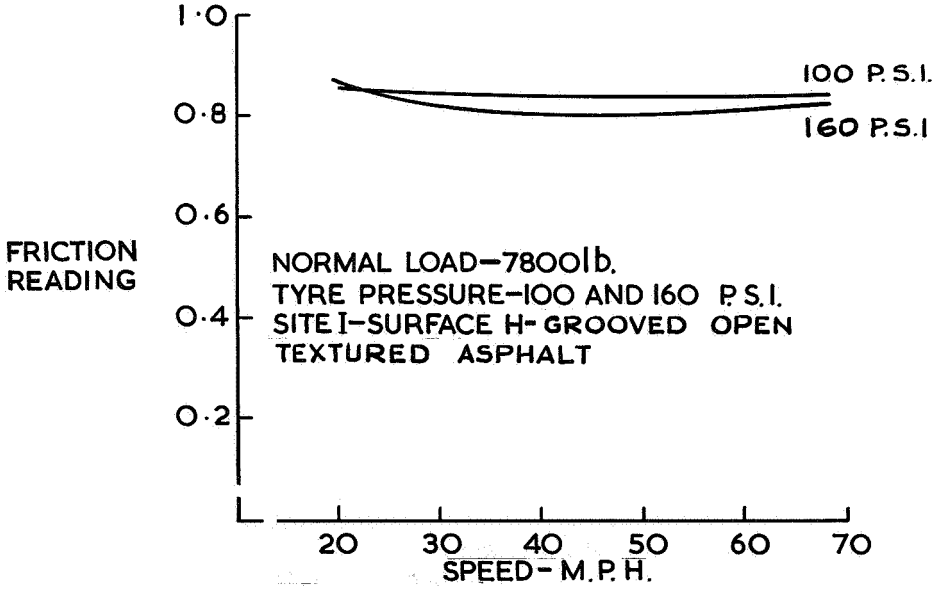

Figure 29.- Relationship between impending-skid braking-force coefficient and speed with Heavy Load Friction Vehicle. Surface H.

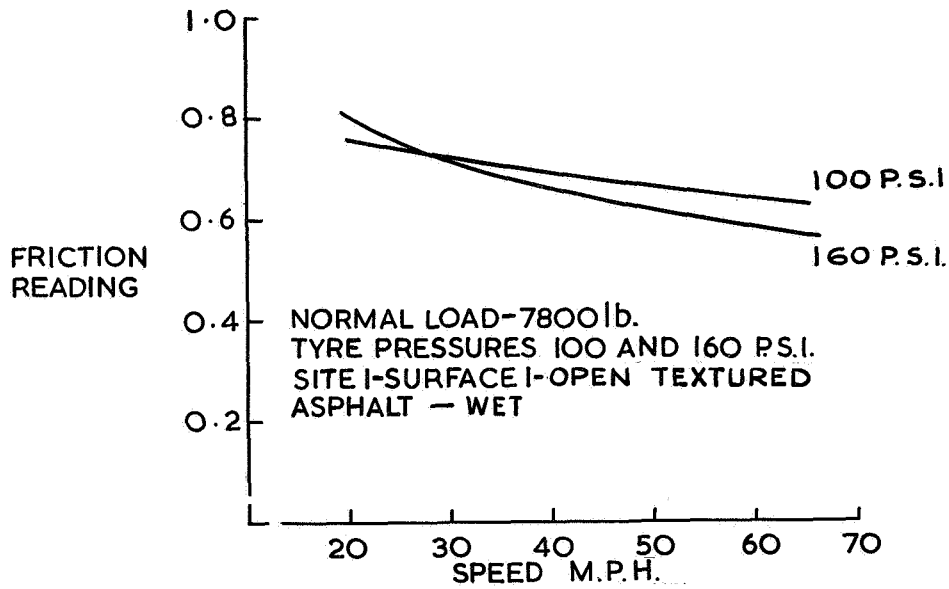

Figure 30.- Relationship between impending-skid braking-force coefficient and speed with Heavy Load Friction Vehicle. Surface I.

1 SITE I–SECTION A – FINE TEXTURED CONCRETE – WET
2 SITE I–SECTION B – GROOVED SMOOTH CONCRETE – WET
3 SITE I–SECTION C – GROOVED TEXTURED CONCRETE–WET
4 SITE I–SECTION D – TEXTURED CONCRETE – WET
5 SITE I–SECTION E – GRIPSTOP – WET
6 SITE I–SECTION F – SMOOTH TEXTURED ASPHALT – WET
7 SITE I–SECTION G – GROOVED SMOOTH ASPHALT – WET
8 SITE I–SECTION H – GROOVED TEXTURED ASPHALT – WET
9 SITE I–SECTION I – TEXTURED ASPHALT – WET
10 SITE I –SECTION C – GROOVED TEXTURED CONCRETE – DRY

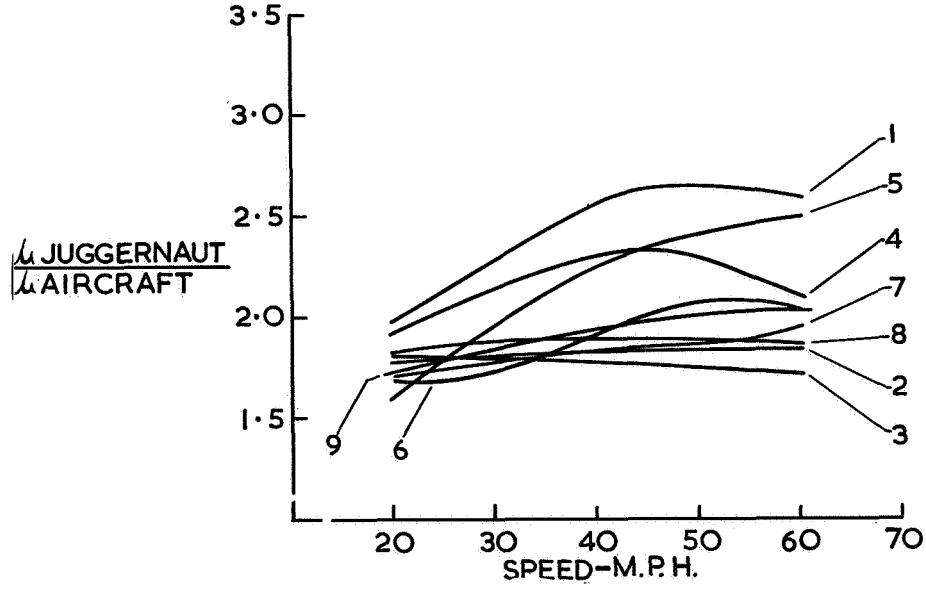

Figure 31.- Correlation between Heavy Load Friction Vehicle and 990 aircraft at 160 psi using anti-skid.

1 SITE 1–SECTION A – FINE TEXTURED CONCRETE – WET
2 SITE 1–SECTION B – GROOVED SMOOTH CONCRETE – WET
3 SITE 1–SECTION C – GROOVED TEXTURED CONCRETE–WET
4 SITE 1–SECTION D – TEXTURED CONCRETE – WET
5 SITE 1–SECTION E – GRIPSTOP – WET
6 SITE 1–SECTION F – SMOOTH TEXTURED ASPHALT – WET
7 SITE 1–SECTION G – GROOVED SMOOTH ASPHALT – WET
8 SITE 1–SECTION H – GROOVED TEXTURED ASPHALT – WET
9 SITE 1–SECTION I – TEXTURED ASPHALT – WET
10 SITE 1 –SECTION C – GROOVED TEXTURED CONCRETE – DRY

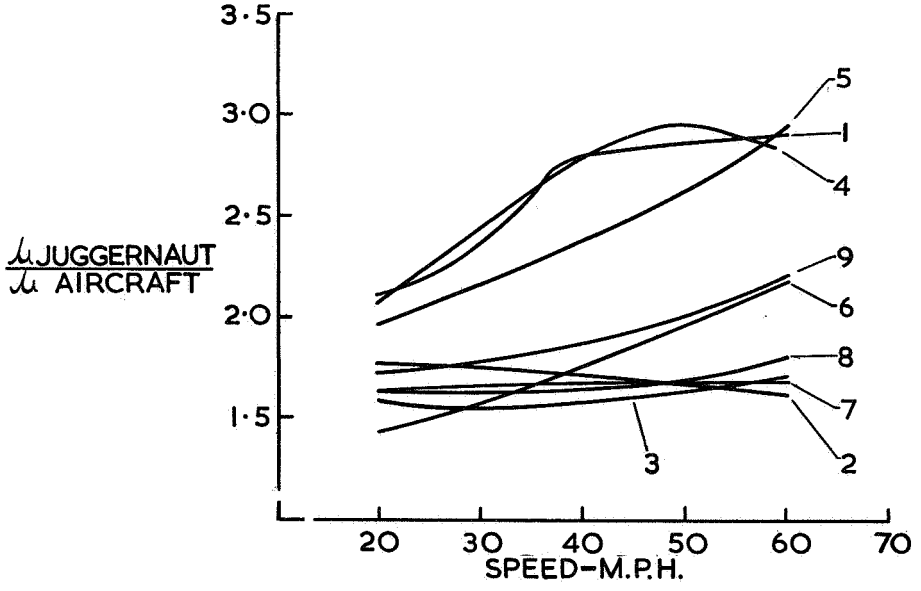

Figure 32.- Correlation between Heavy Load Friction Vehicle at impending skid and 990 aircraft at 160 psi.

1 SITE 1–SECTION A – FINE TEXTURED CONCRETE – WET
2 SITE 1–SECTION B – GROOVED SMOOTH CONCRETE – WET
3 SITE 1–SECTION C – GROOVED TEXTURED CONCRETE–WET
4 SITE 1–SECTION D – TEXTURED CONCRETE – WET
5 SITE 1–SECTION E – GRIPSTOP – WET
6 SITE 1–SECTION F – SMOOTH TEXTURED ASPHALT – WET
7 SITE 1–SECTION G – GROOVED SMOOTH ASPHALT – WET
8 SITE 1–SECTION H – GROOVED TEXTURED ASPHALT – WET
9 SITE 1–SECTION I – TEXTURED ASPHALT – WET
10 SITE 1 –SECTION C – GROOVED TEXTURED CONCRETE – DRY

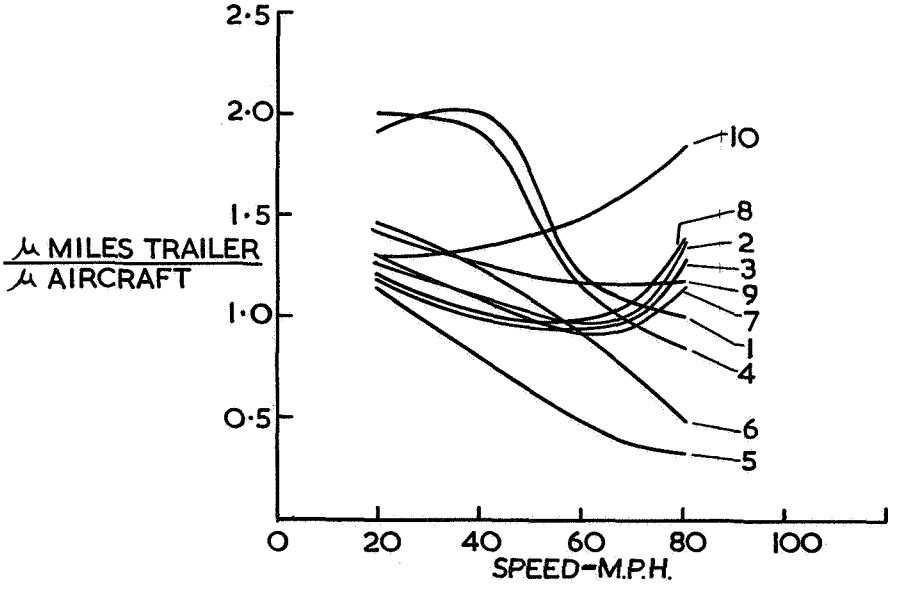

Figure 33.- Correlation between Miles Trailer and 990 aircraft.

1 SITE 1-SECTION A — FINE TEXTURED CONCRETE - WET
2 SITE 1-SECTION B — GROOVED SMOOTH CONCRETE - WET
3 SITE 1-SECTION C — GROOVED TEXTURED CONCRETE - WET
4 SITE 1-SECTION D — TEXTURED CONCRETE - WET
5 SITE 1-SECTION E — GRIPSTOP - WET
6 SITE 1-SECTION F — SMOOTH TEXTURED ASPHALT - WET
7 SITE 1-SECTION G — GROOVED SMOOTH ASPHALT - WET
8 SITE 1-SECTION H — GROOVED TEXTURED ASPHALT - WET
9 SITE 1-SECTION I — TEXTURED ASPHALT - WET
10 SITE 1 -SECTION C — GROOVED TEXTURED CONCRETE - DRY

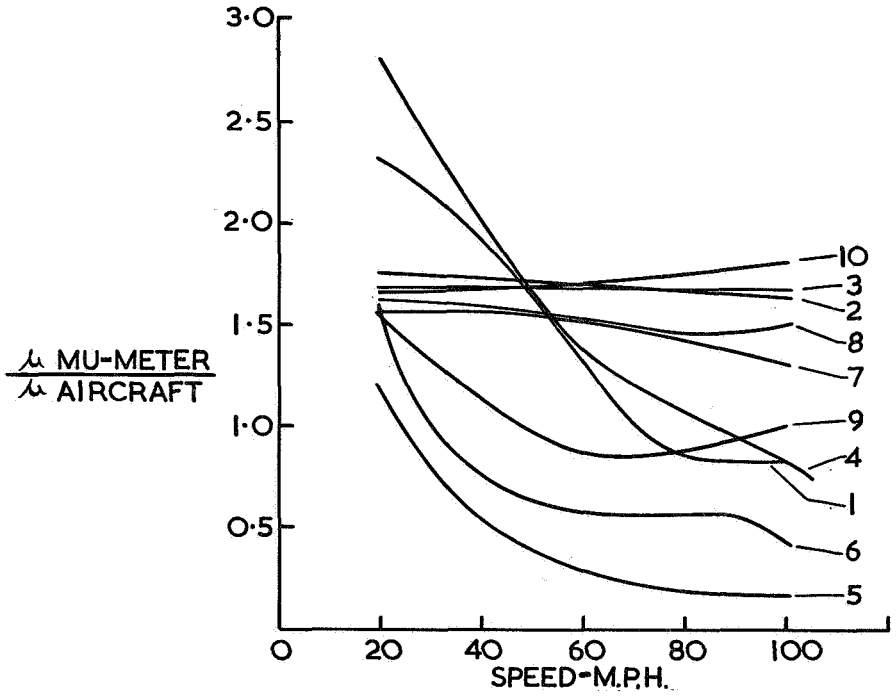

Figure 34.- Correlation between 990 aircraft and Mu-Meter.

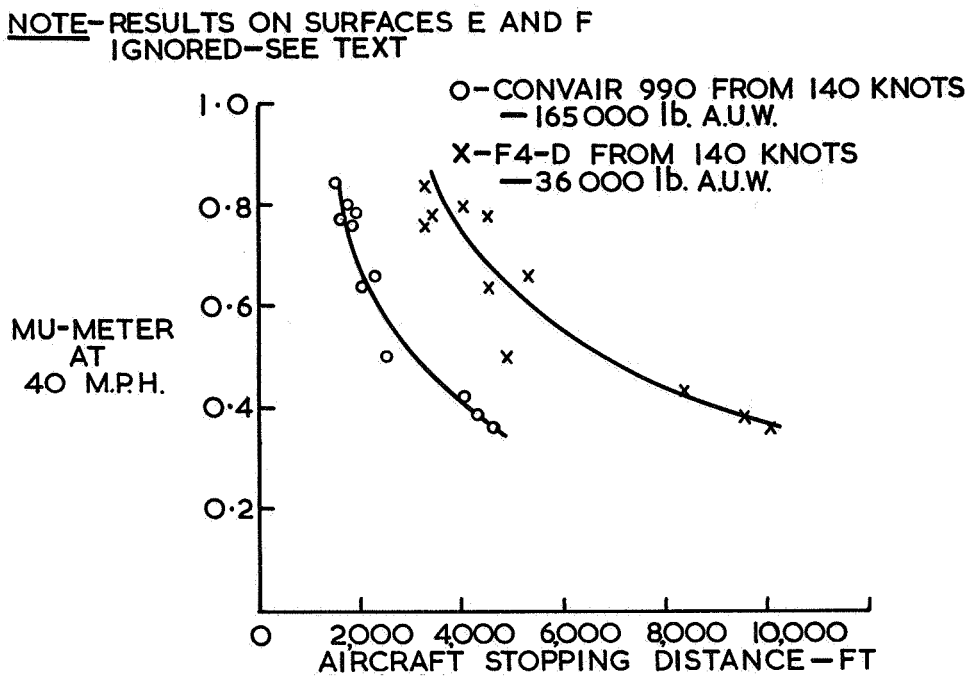

Figure 35.- Mu-Meter correlation with aircraft stopping distances. Site 1.

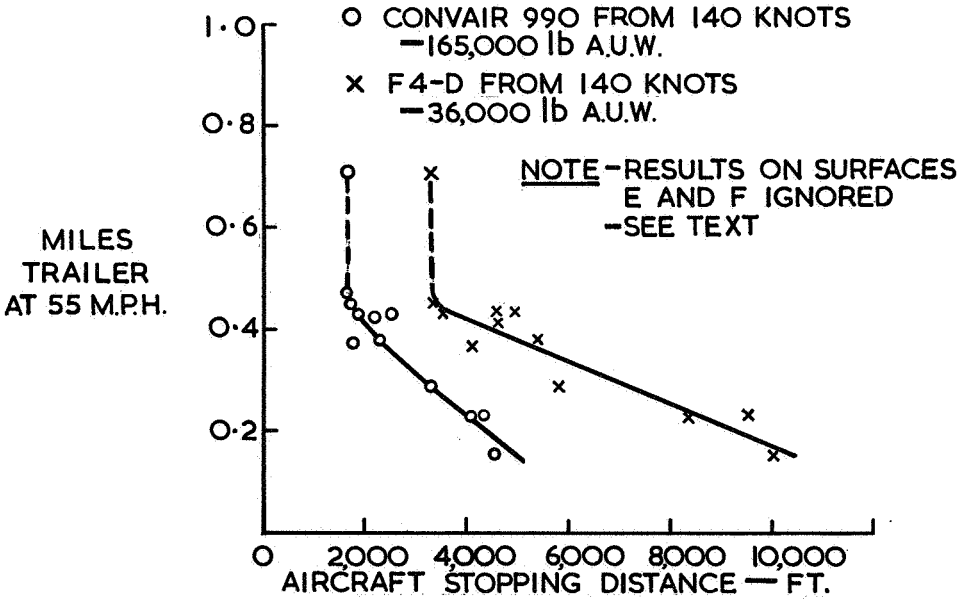

Figure 36.- Miles Trailer correlation with aircraft stopping distances. Site 1.

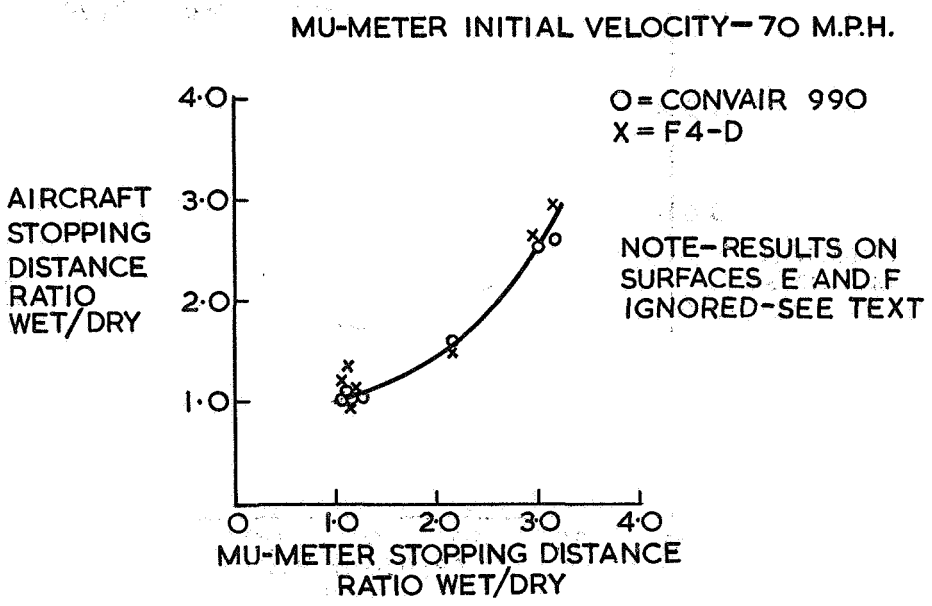

Figure 37.- Use of Mu-Meter stopping distance to indicate aircraft stopping distance.

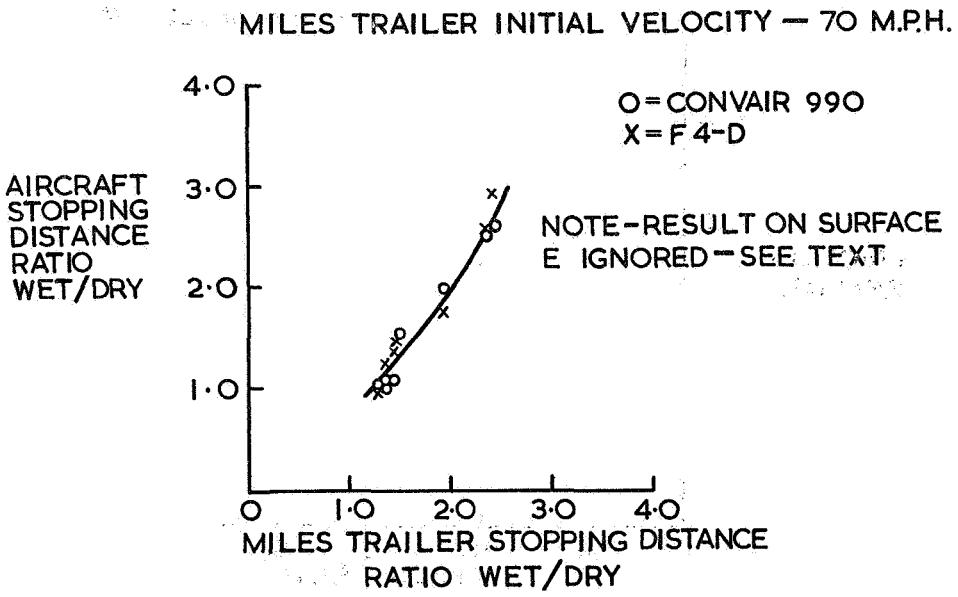

Figure 38.- Use of Miles Trailer stopping distance to indicate aircraft stopping distance.

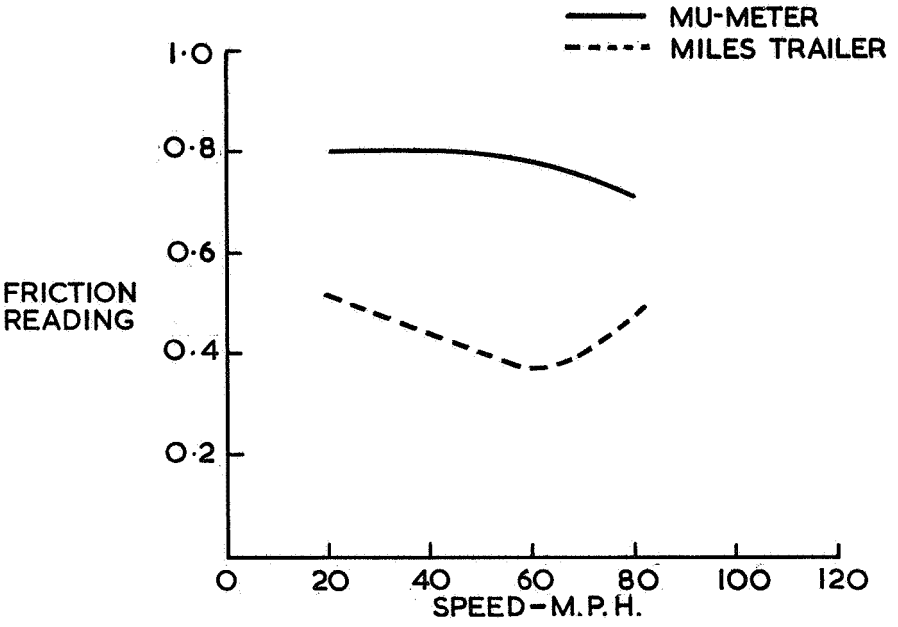

Figure 39.- Site 2, Section 2, Devron epoxy. Grey; wet.

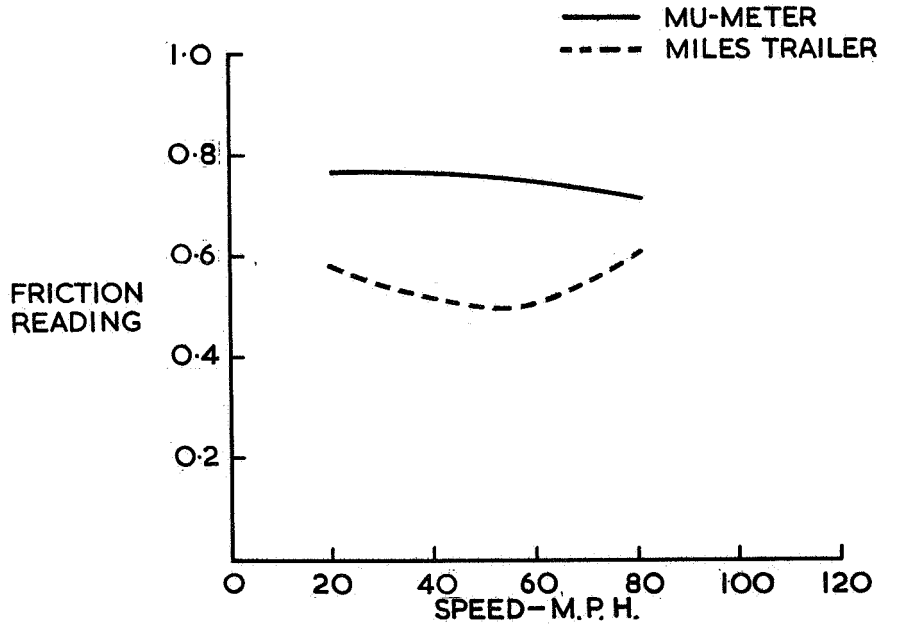

Figure 40.- Site 2, Section 2, original open textured asphalt. Wet.

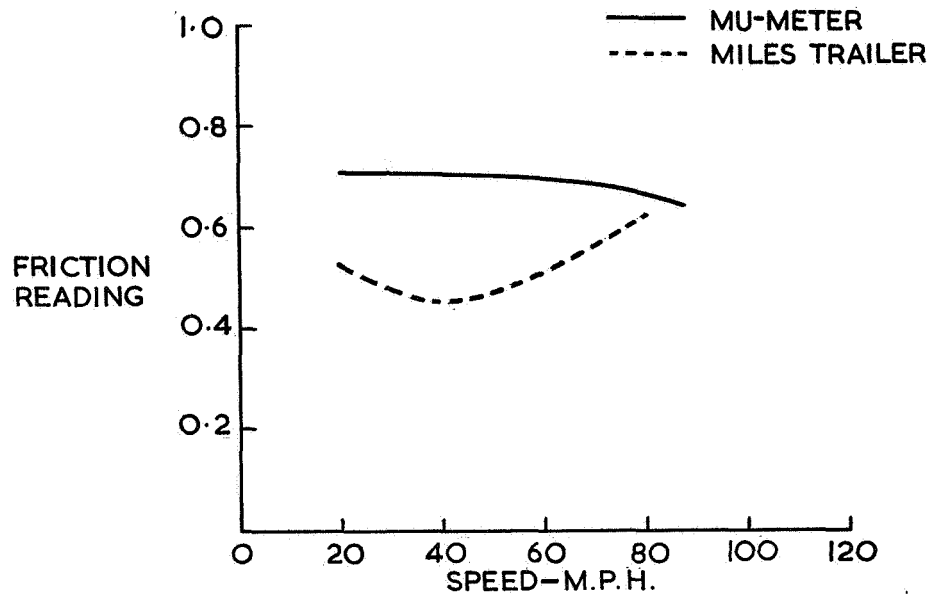

Figure 41.- Site 2, Section 2, transversely grooved concrete, 3/4 by 1/8 by 1/8 inch. Wet.

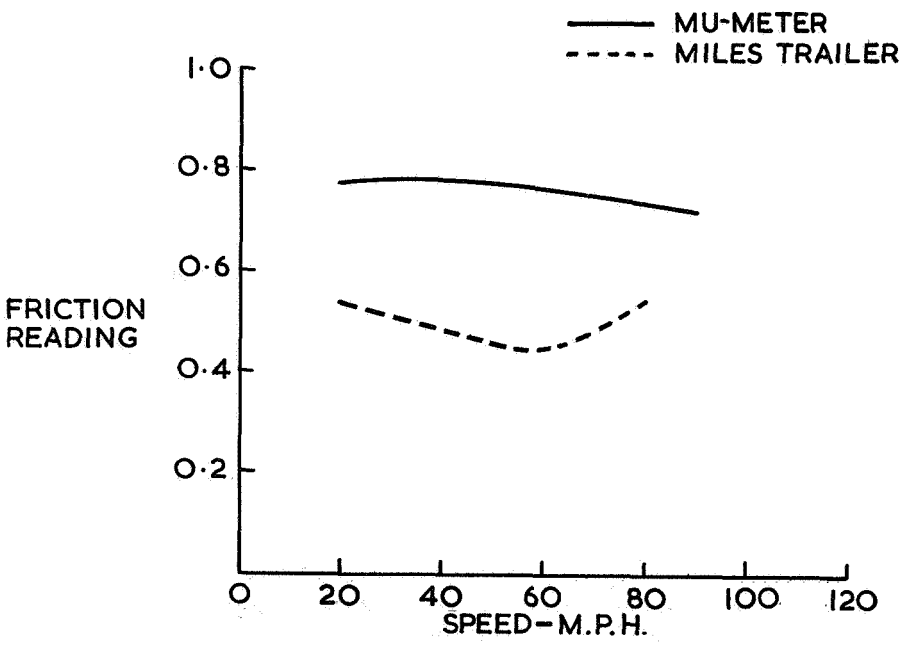

Figure 42.- Site 2, Section 2, transversely grooved asphalt, 3/4 by 1/8 by 1/8 inch. Wet.

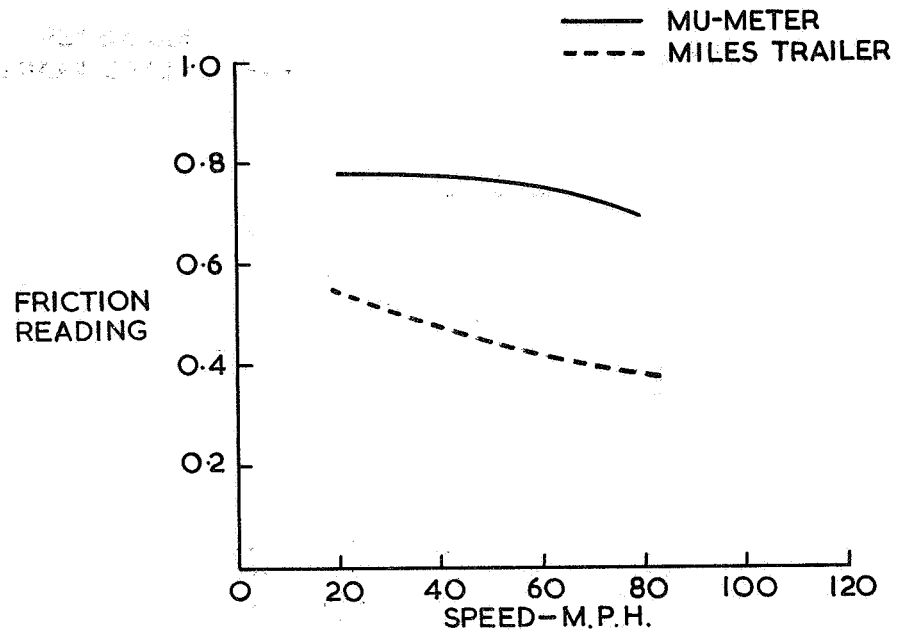

Figure 43.- Site 2, Section 3, epoxy. Wet.

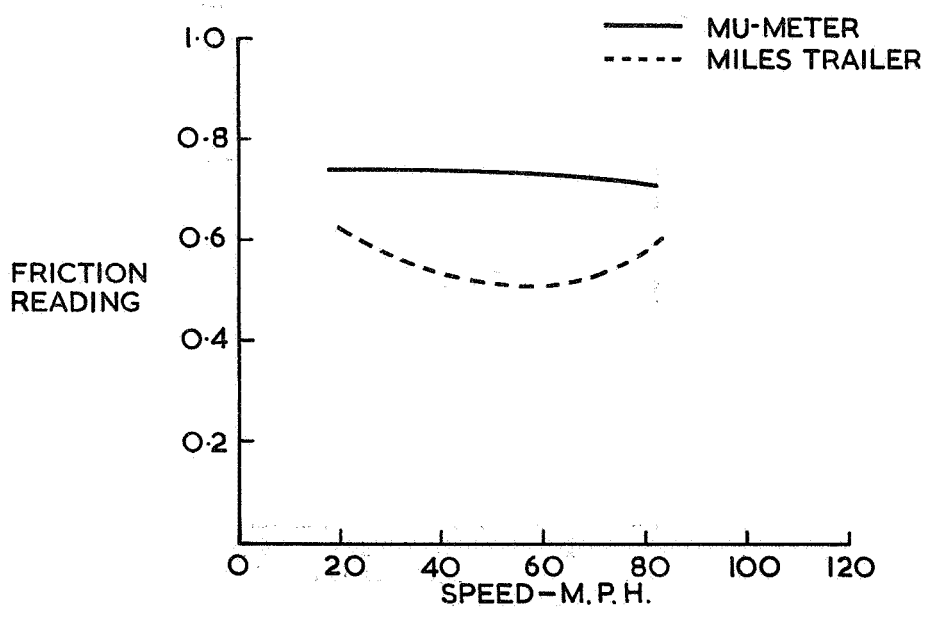

Figure 44.- Site 2, Section 3, original open textured asphalt. Wet.

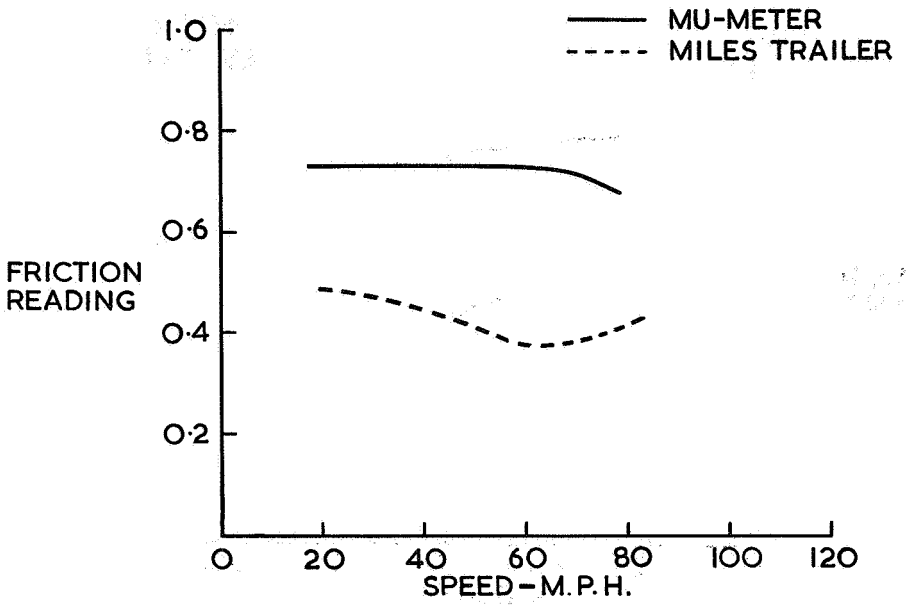

Figure 45.- Site 2, Section 3, concrete with longitudinal grooves, 3/4 by 1/8 by 1/8 inch. Wet.

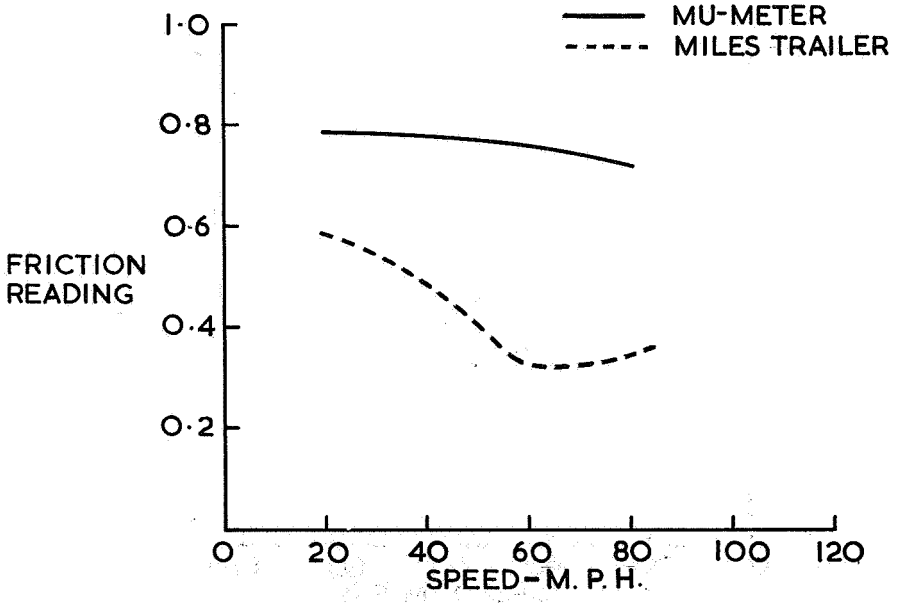

Figure 46.- Site 2, Section 3, asphalt with longitudinal grooves, 3/4 by 1/8 by 1/8 inch. Wet.

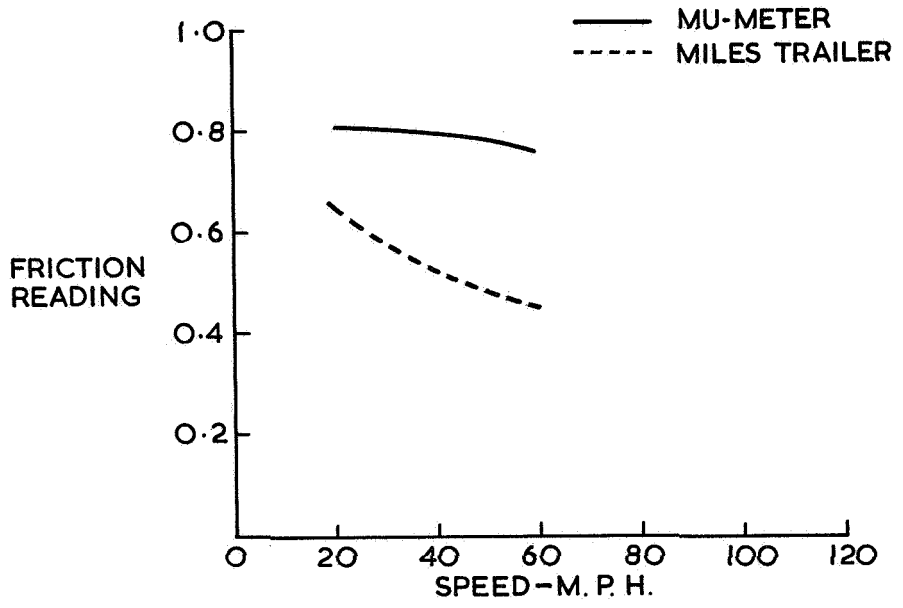

Figure 47.- Site 2, Section 4, Carrier Deck Paint. Wet.

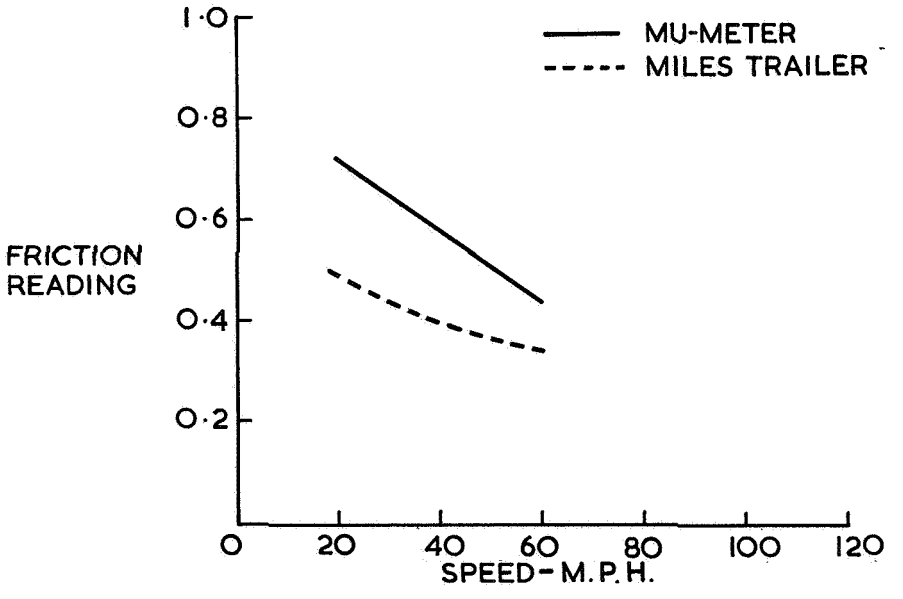

Figure 48.- Site 2, Section 4, fine textured concrete. Wet.

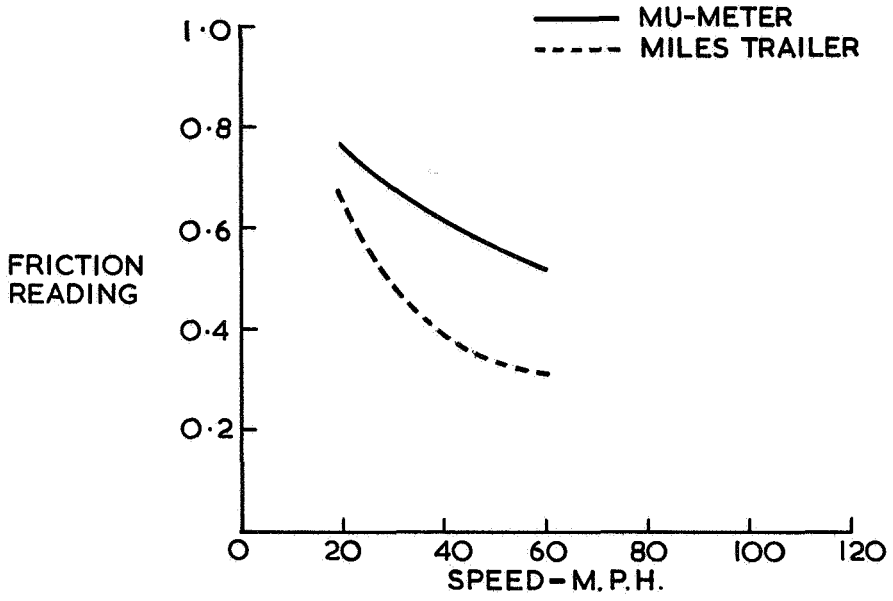

Figure 49.- Site 2, Section 4, longitudinally grooved asphalt, 1 by 1/8 by 1/8 inch. Wet.

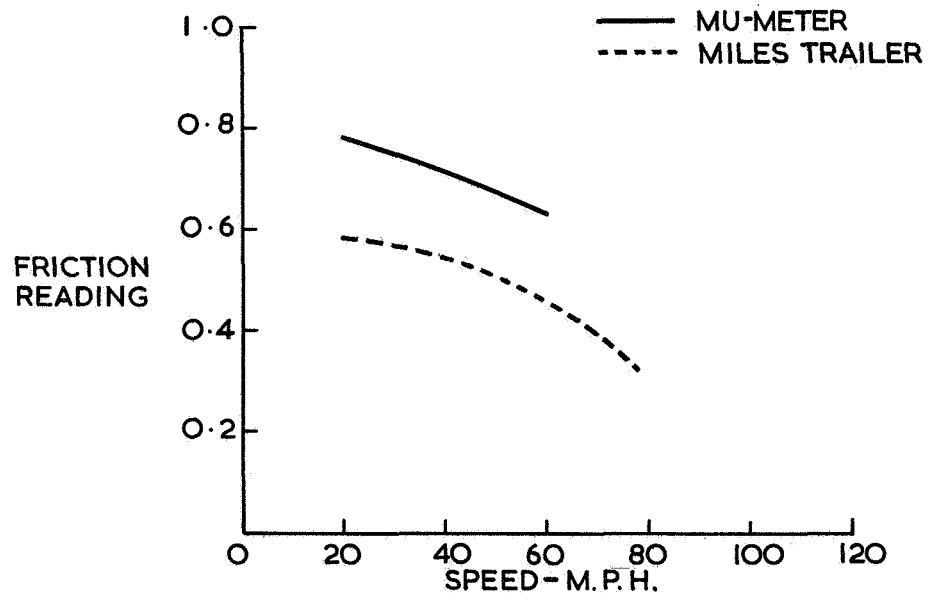

Figure 50.- Site 2, Section 5, Sinopal. Wet.

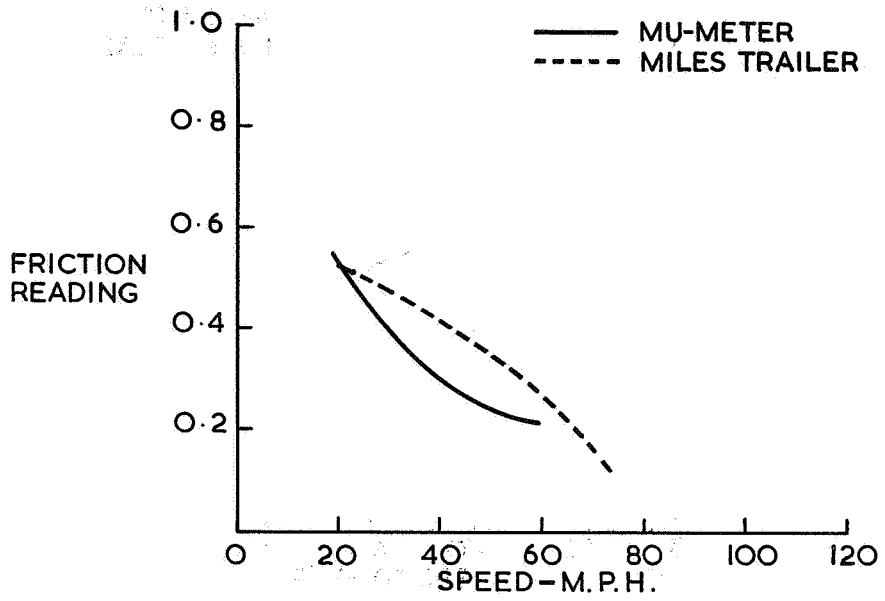

Figure 51.- Site 2, Section 5, Eastern Shore sand mix. Wet.

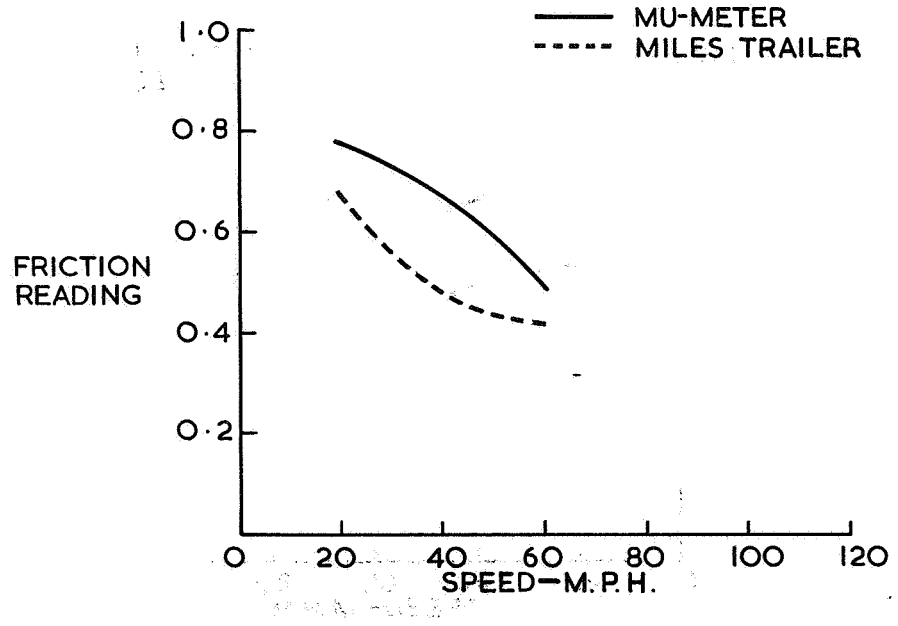

Figure 52.- Site 2, Section 5, transversely grooved asphalt, 1 by 1/8 by 1/8 inch. Wet.

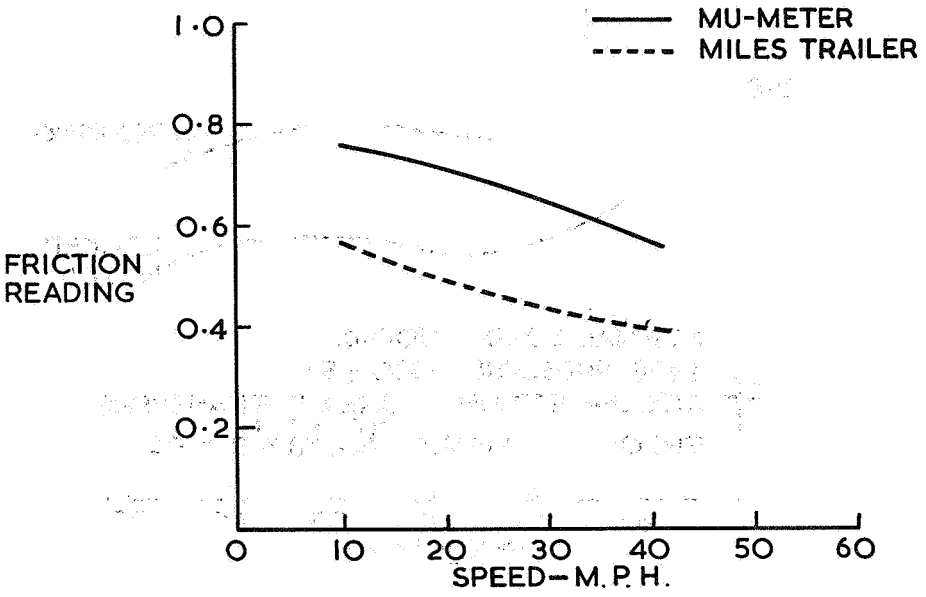

Figure 53.- Site 2, Section 6, fine textured asphalt. Wet.

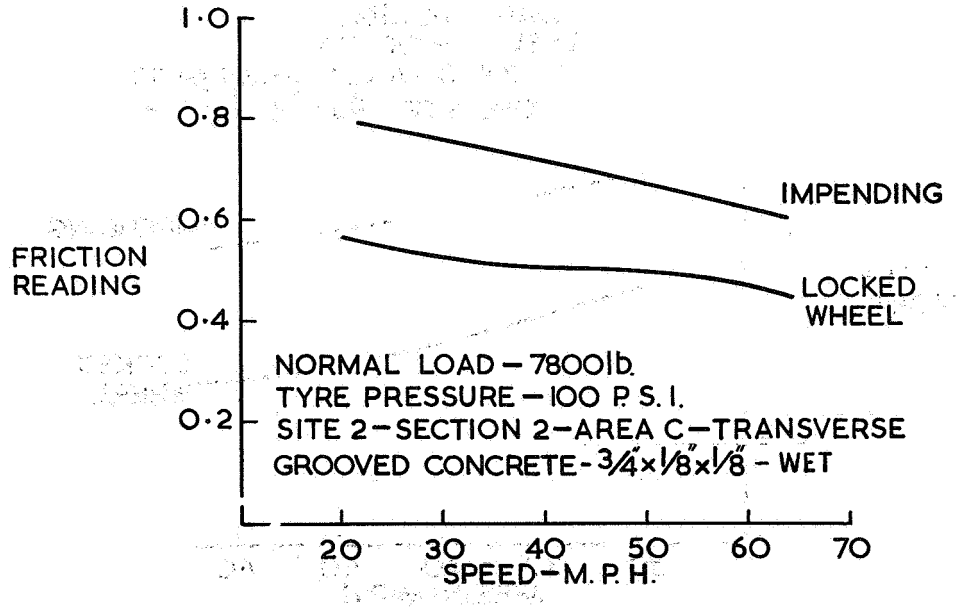

Figure 54.- Relationship between locked-wheel and impending-skid braking-force coefficients and speed with Heavy Load Friction Vehicle. Transversely grooved concrete, 3/4 by 1/8 by 1/8 inch.

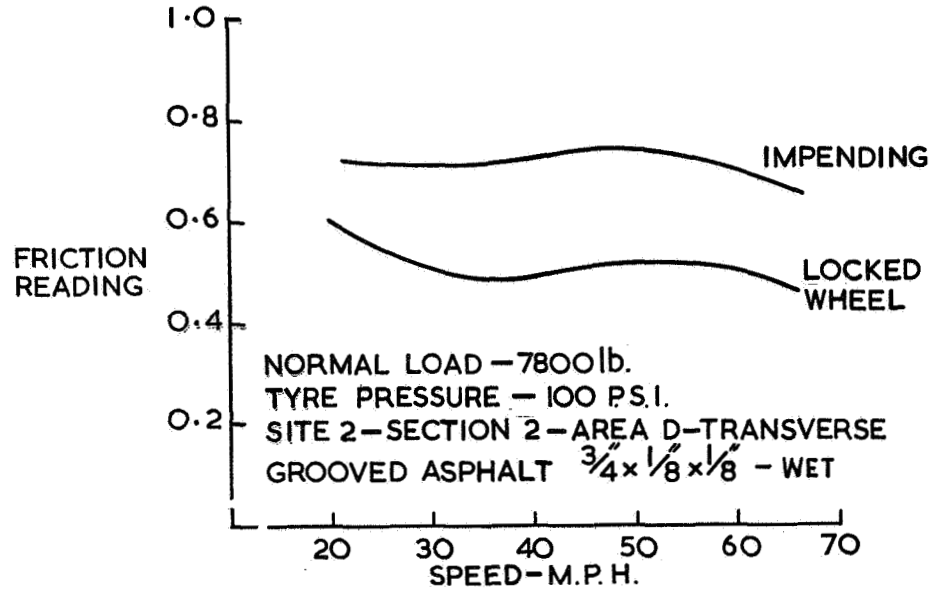

Figure 55.- Relationship between locked-wheel and impending-skid braking-force coefficients with Heavy Load Friction Vehicle. Transversely grooved asphalt, 3/4 by 1/8 by 1/8 inch.

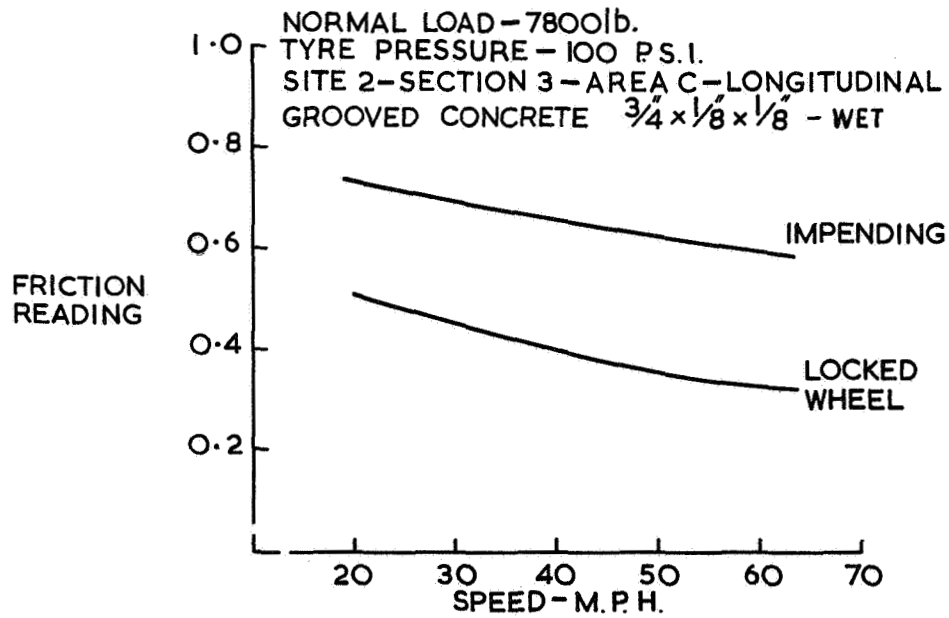

Figure 56.- Relationship between locked-wheel and impending-skid braking-force coefficients with Heavy Load Friction Vehicle. Longitudinally grooved concrete.

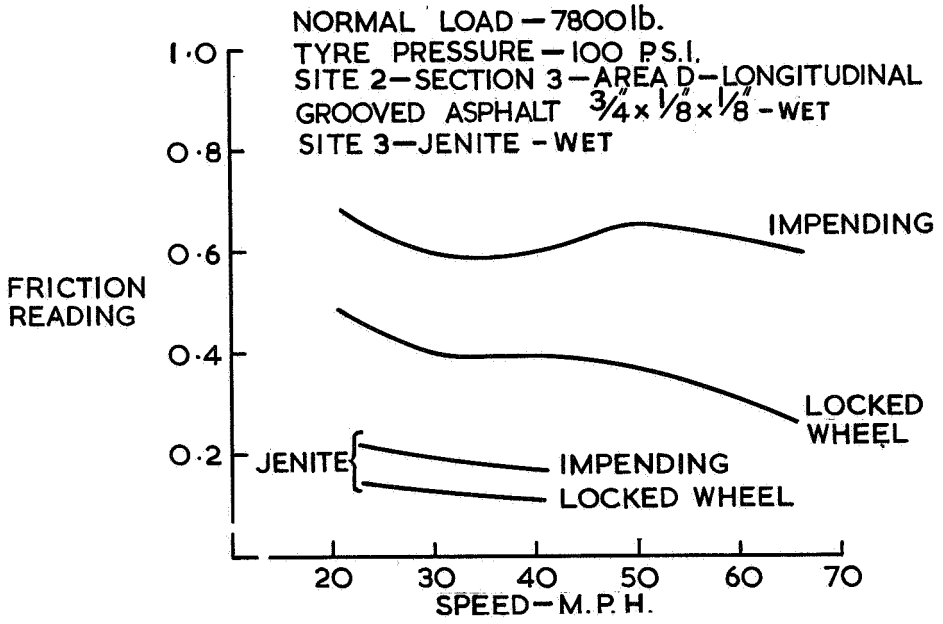

Figure 57.- Relationship between locked-wheel and impending-skid braking-force coefficients with Heavy Load Friction Vehicle. Longitudinally grooved asphalt, 3/4 by 1/8 by 1/8 inch, and Jennite.

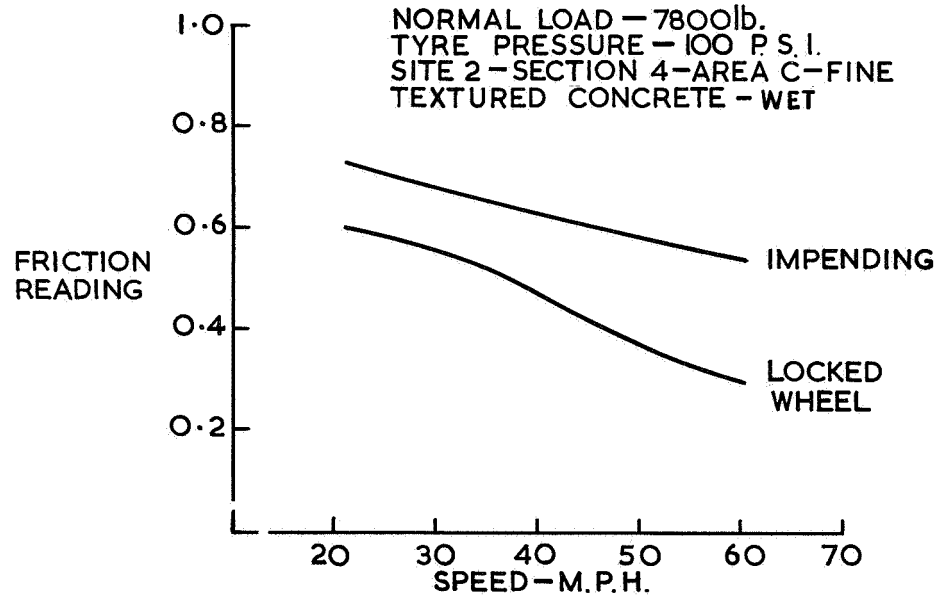

Figure 58.- Relationship between locked-wheel and impending-skid braking-force coefficients with Heavy Load Friction Vehicle. Fine textured concrete.

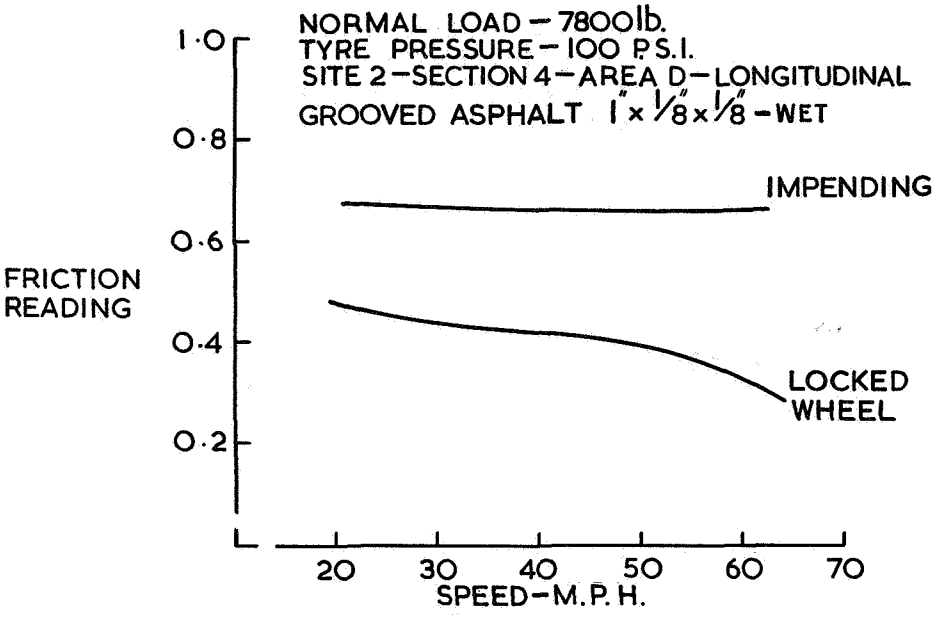

Figure 59.- Relationship between locked-wheel and impending-skid braking-force coefficients with Heavy Load Friction Vehicle. Longitudinally grooved asphalt, 1 by 1/8 by 1/8 inch.

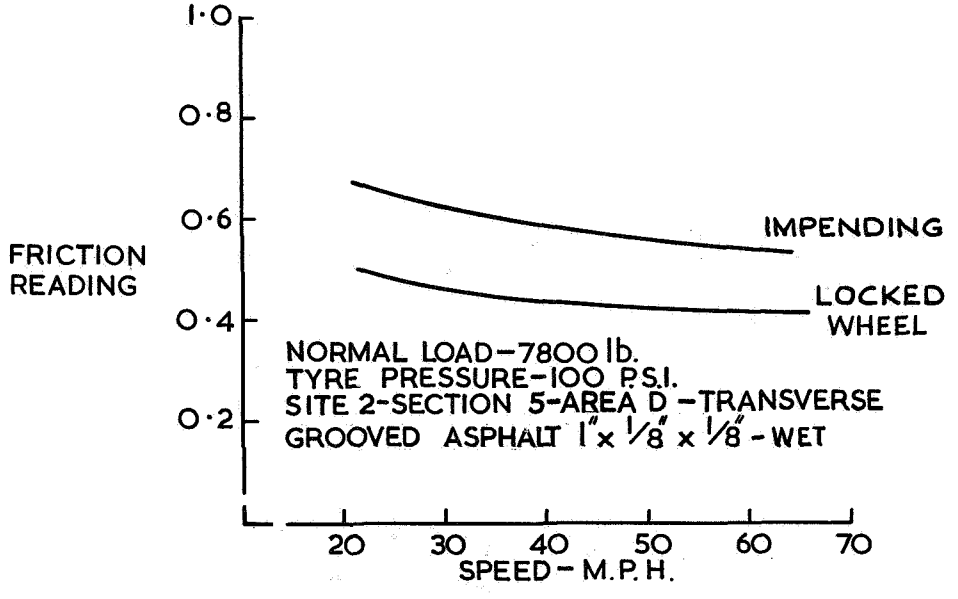

Figure 60.- Relationship between locked-wheel and impending-skid braking-force coefficients with Heavy Load Friction Vehicle. Transversely grooved asphalt, 1 by 1/8 by 1/8 inch.

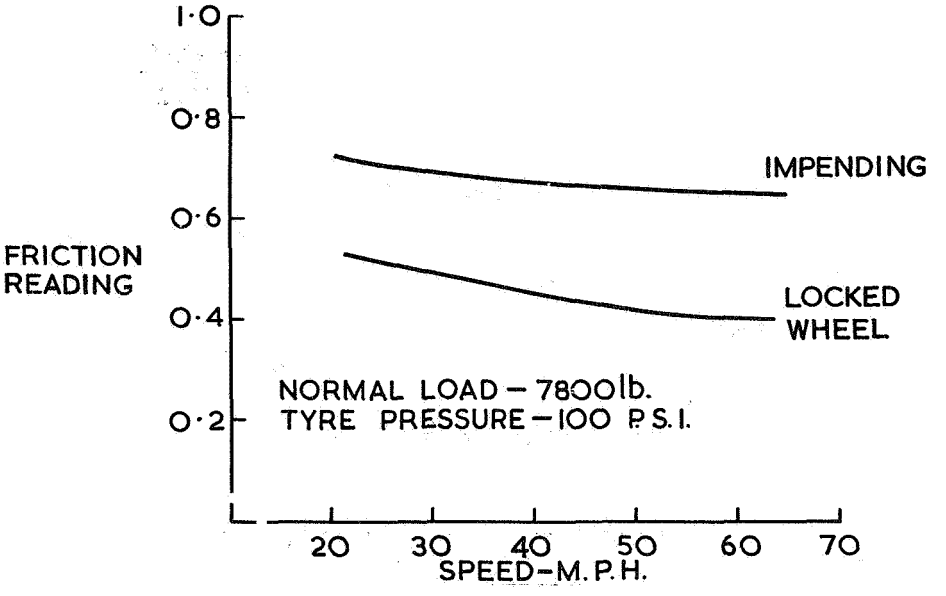

Figure 61.- Relationship between locked-wheel and impending-skid braking-force coefficients with Heavy Load Friction Vehicle. Site 2, Section 5, Sinopal.

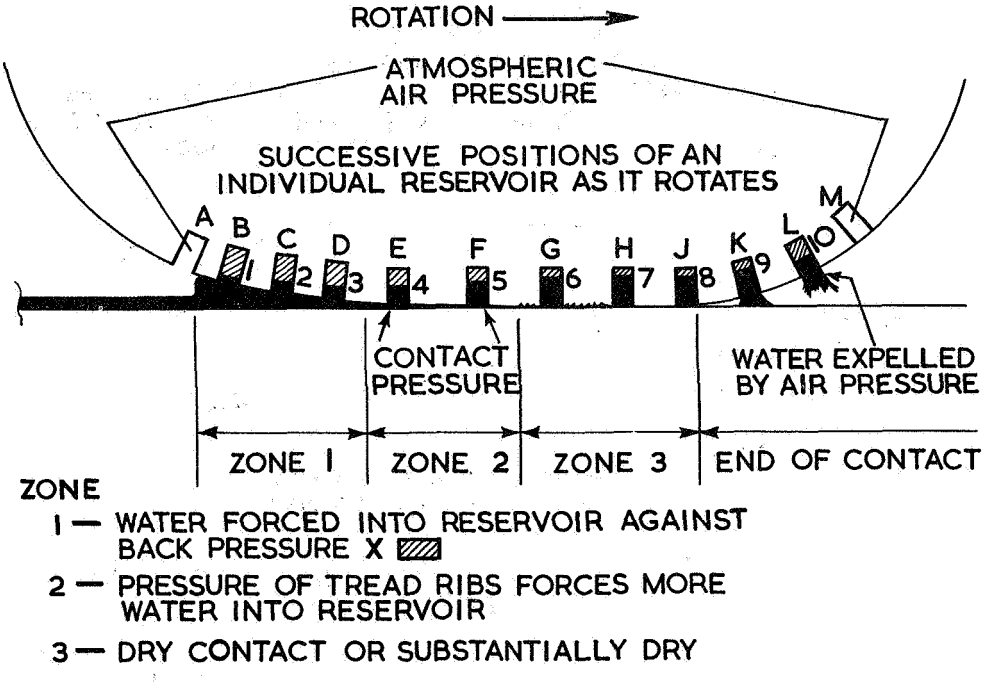

Figure 62.- Dunlop Wet Grip aircraft tyre.

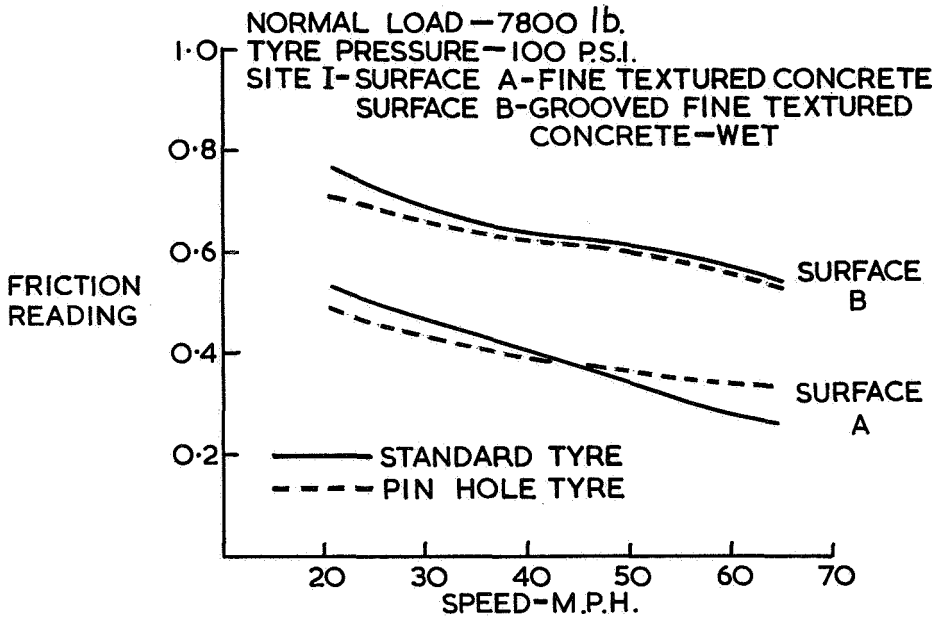

Figure 63.- Relationship between peak value of anti-skid braking-force coefficient and speed with standard and "pin hole" tyres using Heavy Load Friction Vehicle. Surfaces A and B; tyre pressure, 100 psi.

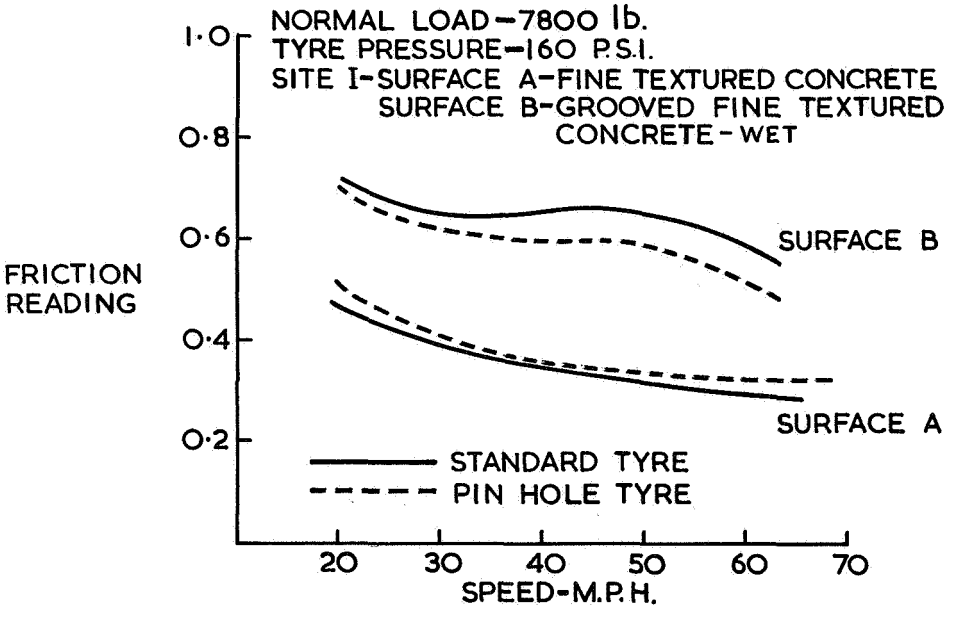

Figure 64.- Relationship between peak value of anti-skid braking-force coefficient and speed with standard and "pin hole" tyres using Heavy Load Friction Vehicle. Surfaces A and B; tyre pressure, 160 psi.

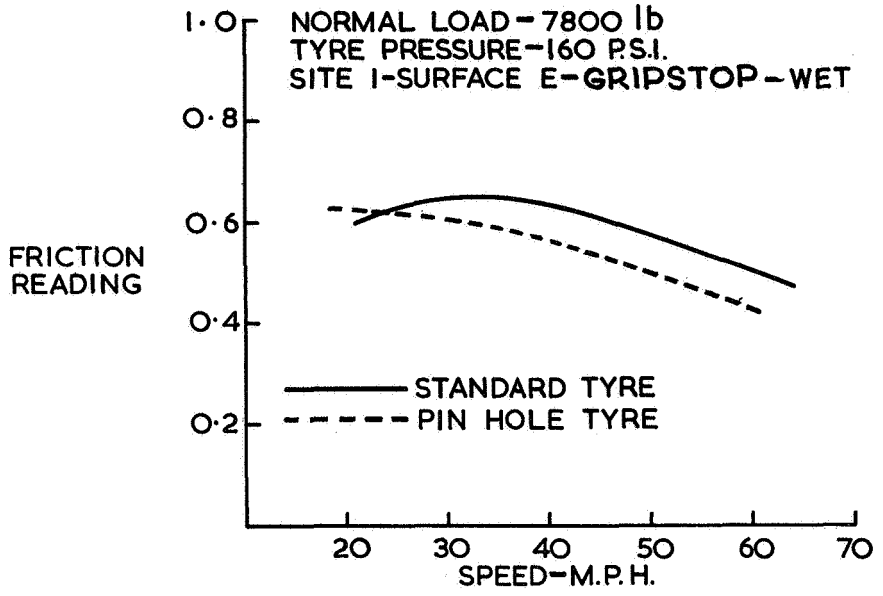

Figure 65.- Relationship between peak value of anti-skid braking-force coefficient and speed with standard and "pin hole" tyres using Heavy Load Friction Vehicle. Surface E.

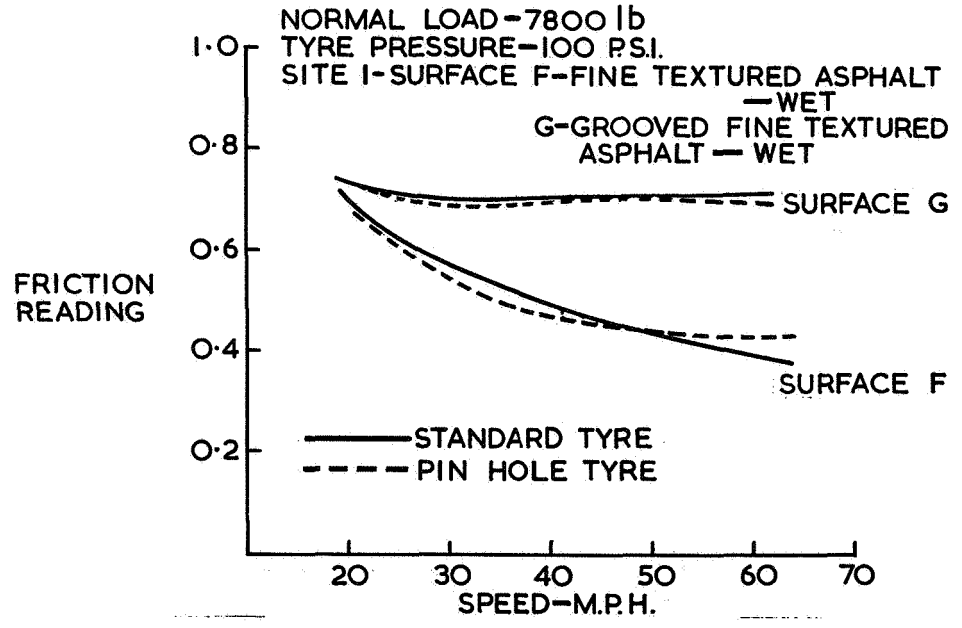

Figure 66.- Relationship between peak value of anti-skid braking-force coefficient and speed with standard and "pin hole" tyres using Heavy Load Friction Vehicle. Surfaces F and G; tyre pressure, 100 psi.

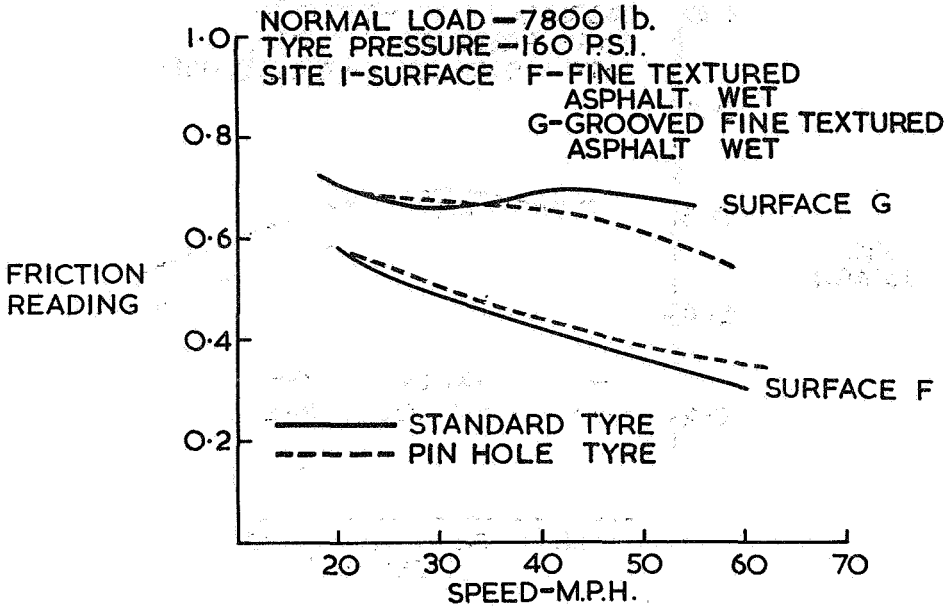

Figure 67.- Relationship between peak value of anti-skid braking-force coefficient and speed with standard and "pin hole" tyres using Heavy Load Friction Vehicle. Surfaces F and G; tyre pressure, 160 psi.

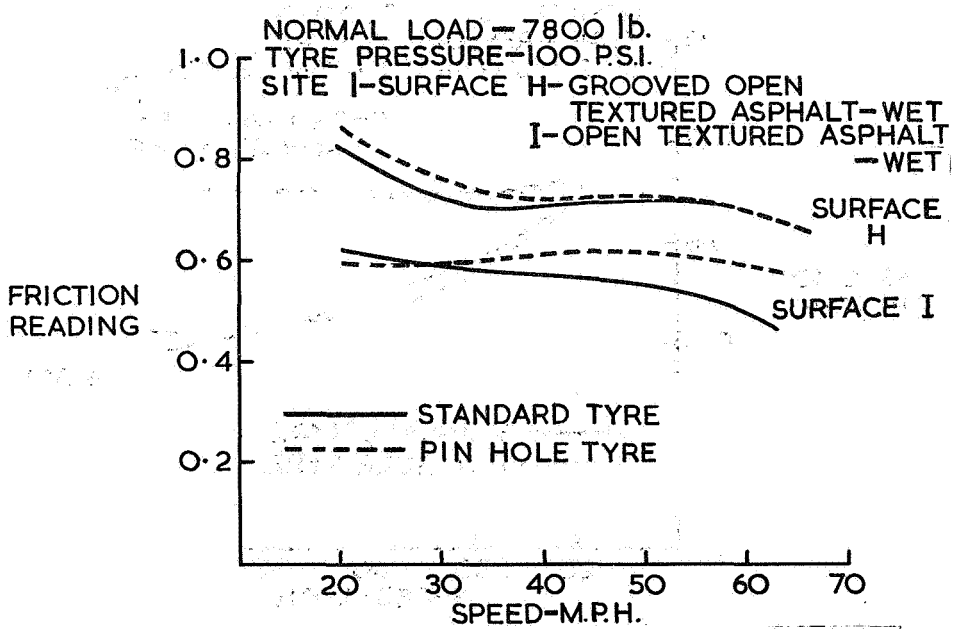

Figure 68.- Relationship between peak value of anti-skid braking-force coefficient and speed with standard and "pin hole" tyres using Heavy Load Friction Vehicle. Surfaces H and I; tyre pressure, 100 psi.

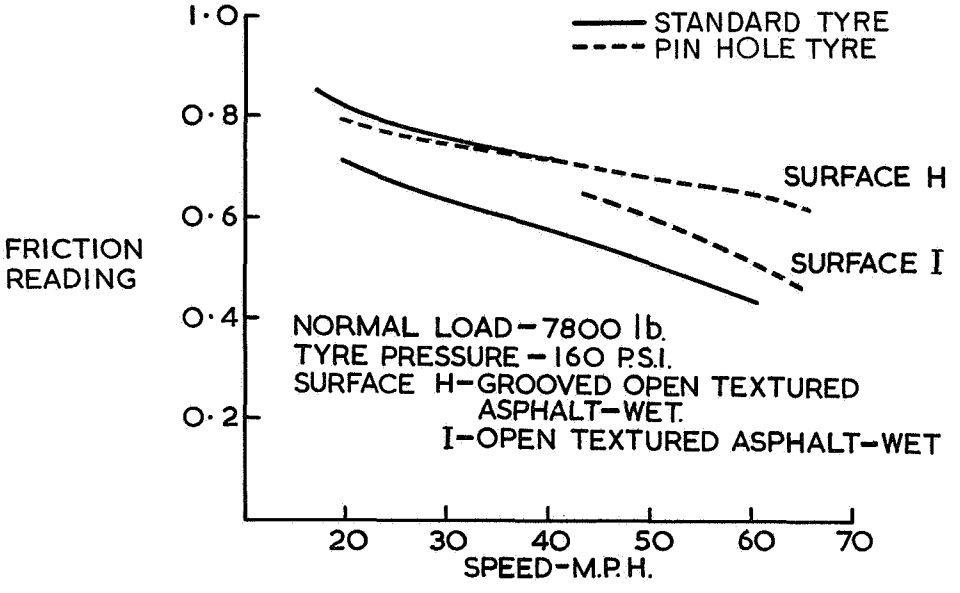

Figure 69.- Relationship between peak value of anti-skid braking-force coefficient and speed with standard and "pin hole" tyres using Heavy Load Friction Vehicle. Surfaces H and I; tyre pressure, 160 psi.